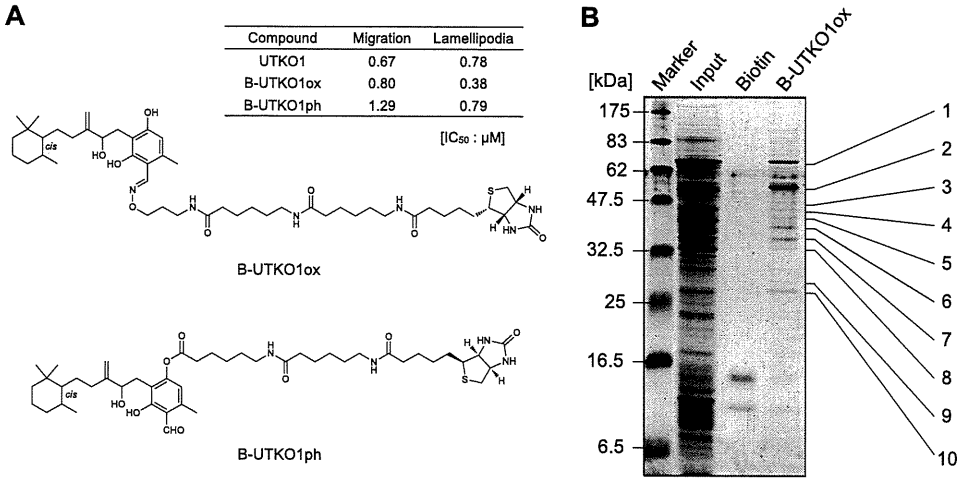

FIGURE 3. **Identification of UTKO1 binding proteins.** *A*, structures and bioactivities of B-UTKO1s. Bioactivities are shown as IC_{50} values in chemotaxis chamber assay and in lamellipodia formation assay. *B*, purification of UTKO1 binding proteins. Lysates of A431 cells stimulated with EGF for 4 h were incubated with biotin (50 nmol) or B-UTKO1ox (50 nmol) and avidin beads overnight. The beads were washed, and co-precipitated proteins were eluted with 2 mM biotin. The eluted proteins were subjected to SDS-PAGE followed by CBB staining. The co-precipitated proteins for B-UTKO1ox were identified as described under "Experimental Procedures."

silencing of Tiam1 expression suppressed in part (50% suppression) the second EGF-induced wave of Rac1 activation, whereas silencing of βPix expression had almost no effect. Furthermore, knockdown of Tiam1 suppressed both the second EGF-induced wave of lamellipodia formation and cell migration (Fig. 5, *C* and *D*). We also showed that Tiam1 is not involved in the first wave of Rac1 activation (supplemental Fig. S4). Similar results were obtained when TT cells were used in place of A431 cells (supplemental Fig. S5). These results demonstrate that Tiam1 is involved in the process of EGF-induced cell migration and therefore might function as the RacGEF responsible for the second EGF-induced wave of Rac1 activation by interacting with 14-3-3ζ.

Because UTKO1 binds to 14-3-3ζ and inhibits Rac1 activation, we examined the possibility that binding of UTKO1 to 14-3-3ζ abrogates the interaction between 14-3-3ζ and Tiam1. Lysates of A431 cells stimulated with EGF for 12 h were incubated with GST-14-3-3ζ in the presence or absence of UTKO1, and Tiam1 that co-precipitated with glutathione-Sepharose 4B was detected by Western blotting using anti-Tiam1 antibody. As shown in Fig. 6*A*, UTKO1 reduced the amount of 14-3-3ζ-bound Tiam1, indicating that it inhibited the interaction between 14-3-3ζ and Tiam1. Inhibition of the interaction between 14-3-3ζ and its binding partner by UTKO1 is not non-specific, because UTKO1 also inhibited the interaction between 14-3-3ζ and βPix but did not affect the interaction between 14-3-3ζ and kinesin. Subsequently, we confirmed the inhibition of the interaction between 14-3-3ζ and Tiam1 by UTKO1 in cultured cells by immunoprecipitation assay. A431 cells stably expressing FLAG-14-3-3ζ (A431/FLAG-14-3-3ζ cells) transiently transfected with Tiam1–6×Myc were stimulated with EGF for 12 h in the presence or absence of UTKO1. The cells were lysed, and the protein complexes that were precipitated with anti-FLAG antibody were detected by Western blotting. As shown in Fig. 6*B*, the amount of Tiam1 bound to FLAG-14-3-3ζ was reduced in a dose-dependent manner following treatment with UTKO1, confirming that UTKO1 directly inhibits the interaction between 14-3-3ζ and Tiam1 through binding to 14-3-3ζ.

DISCUSSION

Exposure of cells to growth factors leads to a variety of cellular responses at different times after stimulation. Some signaling molecules responsible for growth factor-stimulated cellular responses are activated by exposure to growth factor not only acutely, but also at a later time. For example, platelet-derived growth factor activates PI3K and PKC within minutes of stimulation and then again after 3–7 and 5–9 h, respectively (27). In addition, it has been reported that there are two distinct times during G_1 phase when Ras activity is needed for cell cycle progression (28). Moreover, in endothelial cells, biphasic activation of Rac1 has been reported, with the first peak between 1 and 2 h and the second peak at 8 h after induction by wound scratch/IL-1β (29).

We found that EGF induced distinct waves of Rac1 activation. When A431 cells are stimulated with EGF, Rac1 activation begins to wane after 5–20 min as previously reported (12, 16, 18); we also detected a second, prolonged wave of Rac1 activation 6–12 h after EGF stimulation (Fig. 2*A*). The regulation mechanism and role of early EGF-induced Rac1 activation have been extensively studied (12, 18, 30), but the second wave of Rac1 activation has not yet been examined.

UTKO1, an inhibitor of cell migration, was found to inhibit the second EGF-induced wave of Rac1 activation, but not the first wave (Fig. 2, *B–F*). Therefore, UTKO1 provides a useful chemical probe for the elucidation of the regulation mechanism and role of the second wave of Rac1 activation in cell migration. Our first step was to identify the molecular target of UTKO1 as 14-3-3ζ. This conclusion is supported by the following findings: 1) 14-3-3ζ was detected in affinity-purified proteins with biotin-conjugated UTKO1 prepared from lysates of A431 cells stimulated with EGF for 4 h (Figs. 3*B* and 4*A*); 2) biotin-conjugated UTKO1 bound directly to recombinant 14-3-3ζ (Fig. 4*B*); 3) knockdown of 14-3-3ζ by

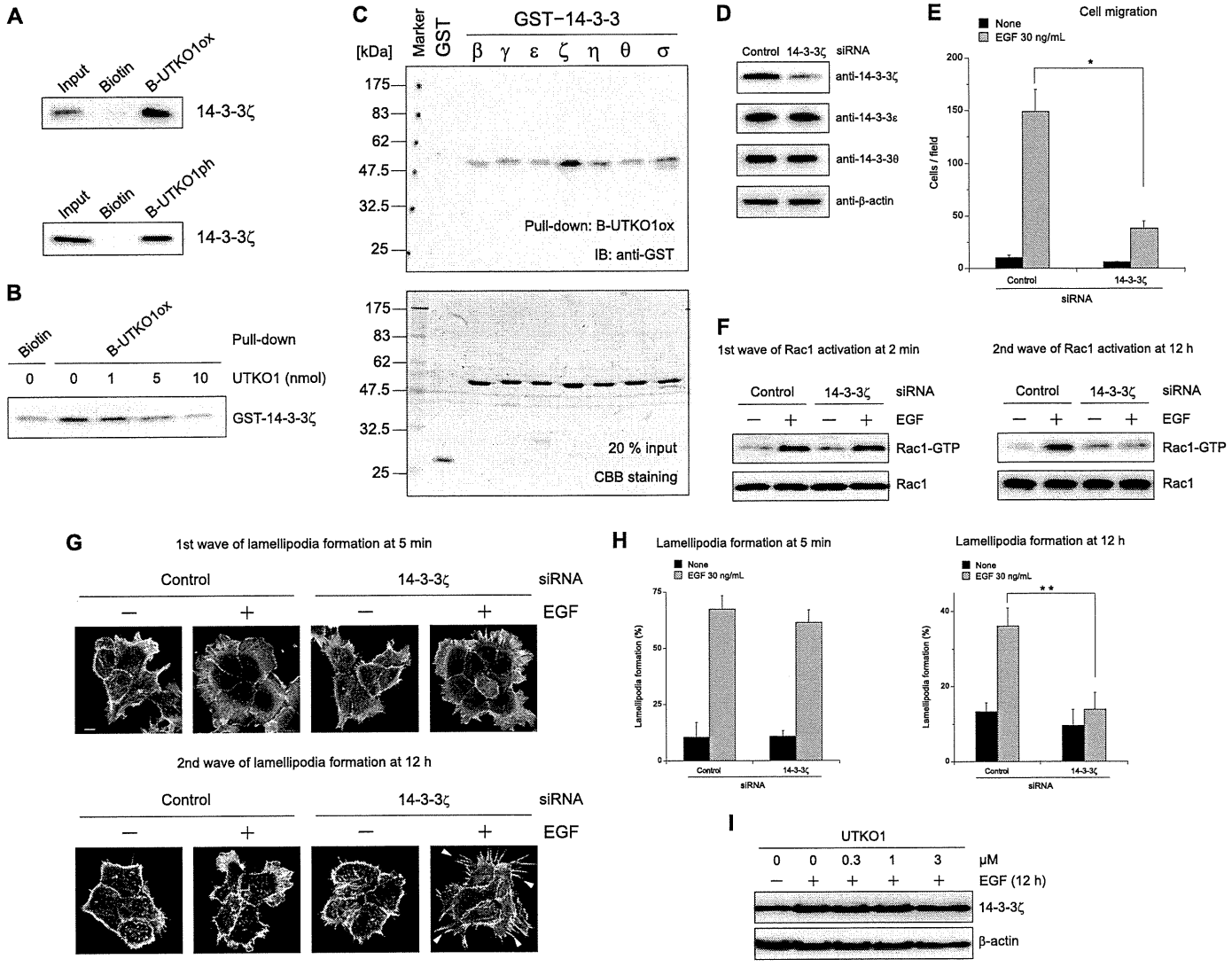

FIGURE 4. **Identification of 14-3-3ζ as a target protein of UTKO1.** *A*, confirmation of the binding of UTKO1 to 14-3-3ζ with Western blotting using anti-14-3-3ζ antibody. *B*, competition assay. Purified GST-tagged 14-3-3ζ (2.5 μg) was preincubated with UTKO1 as a competitor and was treated with biotin (0.5 nmol) or B-UTKO1ox (0.5 nmol) and avidin beads. The precipitated proteins were subjected to Western blotting using anti-GST antibody. *C*, determination of the binding ability of 14-3-3 isoforms to UTKO1. Purified GST or GST-tagged 14-3-3 isoforms were incubated with B-UTKO1ox and avidin beads. The precipitated proteins were subjected to Western blotting using anti-GST antibody (*upper panel*). GST or GST-tagged proteins used for the assay were subjected to SDS-PAGE followed by CBB staining as 20% input (*lower panel*). *D–H*, knockdown experiments. *D*, A431 cells were transfected with control or 14-3-3ζ siRNA and cultured for 72 h. Then the cells were collected and subjected to Western blotting using the indicated antibodies. *E*, control or 14-3-3ζ siRNA-transfected A431 cells were incubated in the upper chamber and stimulated with or without EGF for 24 h, and then the migrated cells were counted. The data represent the means ± S.D. ($n = 5$). *F–H*, control or 14-3-3ζ siRNA-transfected A431 cells were stimulated with EGF for 2 min or 12 h. Then the cells were examined for active Rac1 by pulldown assay (*F*), or the cells were observed under confocal microscopy (*G*), and counted (*H*). *Arrowheads* in *G*, see text. *Scale bar*, 10 μm. The data represent the means ± S.D. ($n = 6$). *I*, effect of UTKO1 on expression levels of 14-3-3ζ protein. A431 cells were pretreated with UTKO1 for 15 min and stimulated with EGF for 12 h. Then the cells were collected and subjected to Western blotting using the indicated antibodies. For *E* and *H*, statistical analyses were performed with a two-tailed Student's *t* test. *, $p = 9.3 \times 10^{-6}$; **, $p = 3.3 \times 10^{-7}$. Throughout, the data were representative of at least three independent studies. For *H*, more than 300 cells were analyzed per experiment. *IB*, immunoblot.

siRNA inhibited the second EGF-induced wave of Rac1 activation but not the first wave (Fig. 4*F*); and 4) the morphology of 14-3-3ζ-deficient A431 cells was very similar to that of UTKO1-treated A431 cells (Figs. 1*F* and 4*G*).

14-3-3ζ belongs to the 14-3-3 protein family, which is a class of highly conserved acidic proteins encoded by seven mammalian genes (α/β, ε, η, γ, τ/θ, ζ/δ, and σ) (21, 22). These seven isoforms share about 50% amino acid identity; nevertheless, UTKO1 seems to bind somewhat selectively to the ζ isomer (Fig. 4*C*). This selectivity can be explained by our finding that UTKO1 bound to the C-terminal region of 14-3-3ζ (supplemental Fig. S3), because this segment is the most variable region of the 14-3-3 isoforms (31). Taken together, these results suggest that 14-3-3ζ is involved in the mechanism for only the second EGF-induced wave of Rac1 activation. Moreover, UTKO1 bound to and inactivated 14-3-3ζ, thereby inhibiting the second EGF-induced wave of Rac1 activation. However, we cannot exclude the possibility that other members of the 14-3-3 family are also related to the inhibition of the second EGF-induced wave of Rac1 activation caused by UTKO1.

What had remained unclear was the mechanism for the involvement of 14-3-3ζ in the second EGF-induced wave of

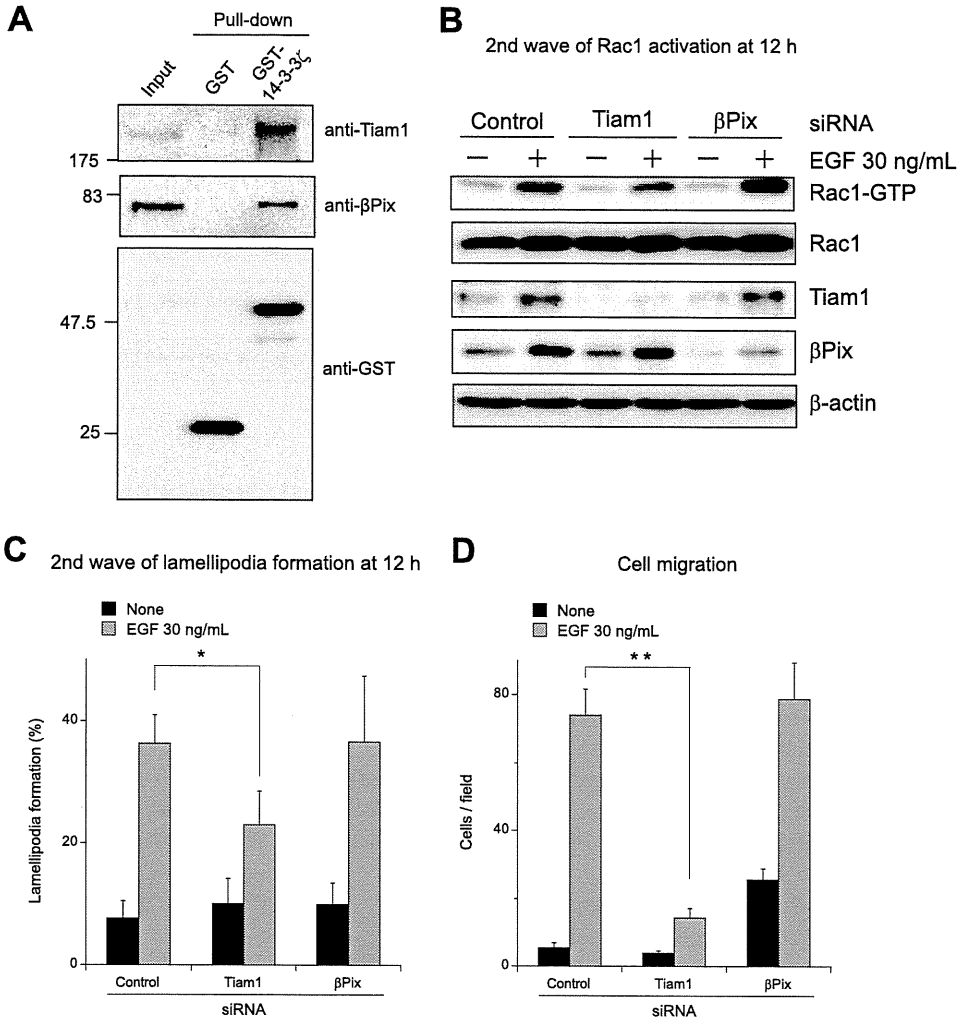

FIGURE 5. **Identification of Tiam1 as a RacGEF which is responsible for the second EGF-induced wave of Rac1 activation.** *A*, GST pulldown assay. Lysates of A431 cells stimulated with EGF for 12 h were incubated with GST or GST-14-3-3ζ and glutathione-Sepharose 4B. The precipitated proteins were subjected to Western blotting using the indicated antibodies. *B–D*, knockdown experiments. *B* and *C*, control, Tiam1, or βPix siRNA-transfected A431 cells were stimulated with EGF for 12 h. Then the cells were examined for active Rac1 by pulldown assay (*B*) or the cells with lamellipodia were counted (*C*). The data represent the means ± S.D. ($n = 6$). *D*, control, Tiam1, or βPix siRNA-transfected A431 cells were incubated in the upper chamber and stimulated with or without EGF for 24 h. Then the migrated cells were counted. The data represent the means ± S.D. ($n = 5$). For *C* and *D*, statistical analyses were performed with a two-tailed Student's *t* test. *, $p = 0.0036$; **, $p = 5.9 \times 10^{-9}$. Throughout, the data were representative of at least three independent studies. For *C*, more than 300 cells were analyzed per experiment.

Rac1 activation and how UTKO1 binding to 14-3-3ζ related to the suppression of the second wave. 14-3-3 proteins function as molecular scaffolds by modulating the conformation of their binding partners; therefore, we speculated that the binding partner of 14-3-3ζ would regulate the second EGF-induced wave of Rac1 activation. Of more than 200 known binding partners of 14-3-3 proteins (25, 32, 33), Tiam1 has been reported to be a Rac-specific GEF (34). Indeed, Tiam1 in lysates from A431 cells stimulated with EGF for 12 h was confirmed to co-precipitate with GST-14-3-3ζ (Fig. 5*A*). Knockdown of Tiam1 by siRNA was found to reduce the second EGF-induced wave of Rac1 activation but not the first wave (Fig. 5*B* and supplemental Fig. S4*A*). Interestingly, the intracellular expression level of Tiam1 is quite low in unstimulated A431 cells; it gradually increased and reached its zenith within 12 h after EGF stimulation (supplemental Fig. S6). These findings might explain why Tiam1 is not involved in the first wave of Rac1 activation. The involvement of Tiam1 in the second wave was further confirmed using NSC23766, a specific inhibitor of Tiam1-mediated activation of Rac1 (35, 36): NSC23766 inhibited both EGF-induced cell migration and second wave of Rac1 activation, but not the first wave (supplemental Fig. S7). Taken together with our finding that knockdown of 14-3-3ζ inhibited the second EGF-induced wave of Rac1 activation but not the first wave, the second wave would require interaction between 14-3-3ζ and Tiam1. This interaction was disrupted by the binding of UTKO1 to 14-3-3ζ (Fig. 6); therefore, UTKO1 inhibited the second wave of Rac1 activation by inhibiting the interaction between 14-3-3ζ and Tiam1.

Recently, it has been reported that the interaction of 14-3-3 proteins with the N terminus of Tiam1 regulates its protein stability (37). However, UTKO1 affected neither the stability of Tiam1 protein nor the intracellular localization of Tiam1 in our assay system (supplemental Fig. S8). Therefore, it is likely that conformational change of Tiam1 caused by interaction with

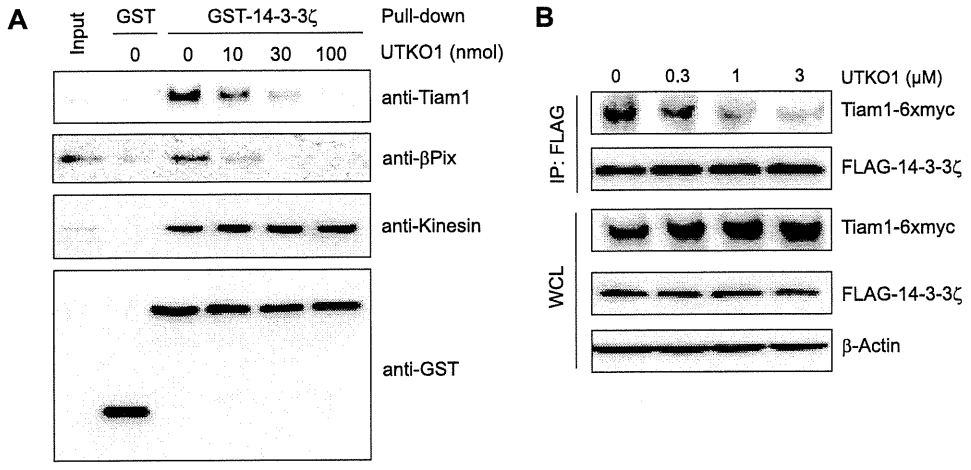

FIGURE 6. **UTKO1 inhibits the binding of 14-3-3ζ to Tiam1.** *A*, GST pulldown assay. Lysates of A431 cells stimulated with EGF for 12 h were incubated with purified GST or GST-14-3-3ζ in the absence or presence of UTKO1. The binding proteins of GST or GST-14-3-3ζ precipitated with glutathione-Sepharose 4B were subjected to Western blotting using the indicated antibodies. *B*, immunoprecipitation assay. FLAG-14-3-3ζ-expressing A431 cells were transiently transfected with Tiam1-6×Myc. After 24 h, the cells were stimulated with EGF for 12 h in the absence or presence of UTKO1. The cells were lysed, and the protein complexes were precipitated with anti-FLAG antibody. The immunoprecipitants were subjected to Western blotting using the indicated antibodies. Throughout, the data were representative of at least three independent studies.

14-3-3ζ activates the GEF property of Tiam1 and is inhibited by UTKO1. However, Tiam1 is not the only GEF regulating the second wave of Rac1 activation, because partial activation of second wave Rac1 was still observed in Tiam1 knockdown A431 cells. Therefore, another RacGEF might be involved in second wave Rac1 activation, possibly also through an interaction with 14-3-3ζ.

βPix, another RacGEF, has also been reported to be a 14-3-3 binding partner (19, 32), and we confirmed the interaction between βPix and 14-3-3ζ. However, knockdown of βPix did not affect the second EGF-induced wave of Rac1 activation but rather enhanced it even when the cells were not stimulated with EGF (Fig. 5*B* and supplemental Fig. S5*C*). Therefore, although UTKO1 disrupted the interaction of 14-3-3ζ with βPix (Fig. 6*A*), this disruption is not responsible for the UTKO1-inhibited second wave of Rac1 activation.

Among the multiple GEFs, Asef and Vav2 have been shown to activate Rac1 in response to EGF (18, 38). However, in most reported experiments, Rac1 activation was detected only within minutes of EGF stimulation (12, 18, 38, 39). We did not detect any interaction between 14-3-3ζ and Asef or Vav2 at times corresponding to the first or second wave following EGF stimulation (supplemental Fig. S9). Therefore, it is likely that Asef and Vav2 function as RacGEF during the first wave of Rac1 activation but are not involved in the 14-3-3ζ-mediated EGF-induced wave of Rac1 activation. Moreover, we cannot exclude the possibility that a 14-3-3 binding partner other than RacGEF is responsible for the second wave of Rac1 activation.

The biphasic timing of Rac1 activation mirrors the biphasic formation of lamellipodia. The first wave of lamellipodia formation seems to be nonpolarized, but second wave lamellipodia are formed at the leading edge and polarized. Moreover, because inhibition of only the second wave of Rac1 activation by UTKO1, as well as NSC23766, is enough to inhibit cell migration, the second wave is required for EGF-induced cell migration. The precise role of each wave of Rac1 activation in EGF-induced cell migration is being actively investigated.

Acknowledgments—We thank Dr. M. Yoshida and Dr. A. Ito for the LC-MS/MS analysis (RIKEN, Japan) and Dr. H. Sugimura for kindly providing plasmid (Hamamatsu University School of Medicine, Japan).

REFERENCES

1. Lauffenburger, D. A., and Horwitz, A. F. (1996) *Cell* **84,** 359–369
2. Pollard, T. D., and Borisy, G. G. (2003) *Cell* **112,** 453–465
3. Small, J. V., Stradal, T., Vignal, E., and Rottner, K. (2002) *Trends Cell Biol.* **12,** 112–120
4. Yamazaki, D., Suetsugu, S., Miki, H., Kataoka, Y., Nishikawa, S., Fujiwara, T., Yoshida, N., and Takenawa, T. (2003) *Nature* **424,** 452–456
5. Blanchoin, L., Amann, K. J., Higgs, H. N., Marchand, J. B., Kaiser, D. A., and Pollard, T. D. (2000) *Nature* **404,** 1007–1011
6. Takenawa, T., and Miki, H. (2001) *J. Cell Sci.* **114,** 1801–1809
7. Ridley, A. J., and Hall, A. (1992) *Cell* **70,** 389–399
8. Nobes, C. D., and Hall, A. (1995) *Cell* **81,** 53–62
9. Ridley, A. J., Paterson, H. F., Johnston, C. L., Diekmann, D., and Hall, A. (1992) *Cell* **70,** 401–410
10. Kaibuchi, K., Kuroda, S., and Amano, M. (1999) *Annu. Rev. Biochem.* **68,** 459–486
11. Takai, Y., Sasaki, T., and Matozaki, T. (2001) *Physiol. Rev.* **81,** 153–208
12. Kurokawa, K., Itoh, R. E., Yoshizaki, H., Nakamura, Y. O., and Matsuda, M. (2004) *Mol. Biol. Cell* **15,** 1003–1010
13. Takemoto, Y., Watanabe, H., Uchida, K., Matsumura, K., Nakae, K., Tashiro, E., Shindo, K., Kitahara, T., and Imoto, M. (2005) *Chem. Biol.* **12,** 1337–1347
14. Sawada, M., Kubo, S., Matsumura, K., Takemoto, Y., Kobayashi, H., Tashiro, E., Kitahara, T., Watanabe, H., and Imoto, M. (2011) *Bioorg. Med. Chem. Lett.* **21,** 1385–1389
15. Jones, G. E., Allen, W. E., and Ridley, A. J. (1998) *Cell Adhes. Commun.* **6,** 237–245
16. Chinkers, M., McKanna, J. A., and Cohen, S. (1979) *J. Cell Biol.* **83,** 260–265
17. Burridge, K., and Wennerberg, K. (2004) *Cell* **116,** 167–179
18. Itoh, R. E., Kiyokawa, E., Aoki, K., Nishioka, T., Akiyama, T., and Matsuda, M. (2008) *J. Cell Sci.* **121,** 2635–2642
19. Angrand, P. O., Segura, I., Völkel, P., Ghidelli, S., Terry, R., Brajenovic, M.,

Vintersten, K., Klein, R., Superti-Furga, G., Drewes, G., Kuster, B., Bouwmeester, T., and Acker-Palmer, A. (2006) *Mol. Cell Proteomics* **5,** 2211–2227
20. Deakin, N. O., Bass, M. D., Warwood, S., Schoelermann, J., Mostafavi-Pour, Z., Knight, D., Ballestrem, C., and Humphries, M. J. (2009) *J. Cell Sci.* **122,** 1654–1664
21. Aitken, A., Jones, D., Soneji, Y., and Howell, S. (1995) *Biochem. Soc. Trans.* **23,** 605–611
22. Rittinger, K., Budman, J., Xu, J., Volinia, S., Cantley, L. C., Smerdon, S. J., Gamblin, S. J., and Yaffe, M. B. (1999) *Mol. Cell* **4,** 153–166
23. Biyasheva, A., Svitkina, T., Kunda, P., Baum, B., and Borisy, G. (2004) *J. Cell Sci.* **117,** 837–848
24. van Hemert, M. J., Steensma, H. Y., and van Heusden, G. P. (2001) *Bioessays* **23,** 936–946
25. Pozuelo Rubio, M., Geraghty, K. M., Wong, B. H., Wood, N. T., Campbell, D. G., Morrice, N., and Mackintosh, C. (2004) *Biochem. J.* **379,** 395–408
26. O'Toole, T. E., Bialkowska, K., Li, X., and Fox, J. E. (2011) *J. Cell Physiol.* **226,** 2965–2978
27. Jones, S. M., and Kazlauskas, A. (2001) *Nat. Cell Biol.* **3,** 165–172
28. Jones, S. M., Klinghoffer, R., Prestwich, G. D., Toker, A., and Kazlauskas, A. (1999) *Curr. Biol.* **9,** 512–521
29. Lee, S. H., Kunz, J., Lin, S. H., and Yu-Lee, L. Y. (2007) *Cancer Res.* **67,** 11045–11053
30. Koivusalo, M., Welch, C., Hayashi, H., Scott, C. C., Kim, M., Alexander, T., Touret, N., Hahn, K. M., and Grinstein, S. (2010) *J. Cell Biol.* **188,** 547–563
31. Gardino, A. K., Smerdon, S. J., and Yaffe, M. B. (2006) *Semin. Cancer Biol.* **16,** 173–182
32. Jin, J., Smith, F. D., Stark, C., Wells, C. D., Fawcett, J. P., Kulkarni, S., Metalnikov, P., O'Donnell, P., Taylor, P., Taylor, L., Zougman, A., Woodgett, J. R., Langeberg, L. K., Scott, J. D., and Pawson, T. (2004) *Curr. Biol.* **14,** 1436–1450
33. Meek, S. E., Lane, W. S., and Piwnica-Worms, H. (2004) *J. Biol. Chem.* **279,** 32046–32054
34. Habets, G. G., Scholtes, E. H., Zuydgeest, D., van der Kammen, R. A., Stam, J. C., Berns, A., and Collard, J. G. (1994) *Cell* **77,** 537–549
35. Gao, Y., Dickerson, J. B., Guo, F., Zheng, J., and Zheng, Y. (2004) *Proc. Natl. Acad. Sci. U.S.A.* **101,** 7618–7623
36. Veluthakal, R., Madathilparambil, S. V., McDonald, P., Olson, L. K., and Kowluru, A. (2009) *Biochem. Pharmacol.* **77,** 101–113
37. Woodcock, S. A., Jones, R. C., Edmondson, R. D., and Malliri, A. (2009) *J. Proteome Res.* **8,** 5629–5641
38. Marcoux, N., and Vuori, K. (2003) *Oncogene* **22,** 6100–6106
39. Sini, P., Cannas, A., Koleske, A. J., Di Fiore, P. P., and Scita, G. (2004) *Nat. Cell Biol.* **6,** 268–274

The Journal of Antibiotics (2011) 64, 361–366

www.nature.com/ja

ORIGINAL ARTICLE

Mycotrienin II, a translation inhibitor that prevents ICAM-1 expression induced by pro-inflammatory cytokines

Yuriko Yamada[1], Etsu Tashiro[2], Shigeru Taketani[1], Masaya Imoto[2] and Takao Kataoka[1]

Pro-inflammatory cytokines, such as tumor necrosis factor (TNF)-α and interleukin-1α (IL-1α), trigger the activation of the transcription factor nuclear factor-κB, a molecule that induces the expression of a variety of genes, including intercellular adhesion molecule-1 (ICAM-1). Here, we report that mycotrienin II, a member of the triene-ansamycin group, inhibited the cell-surface ICAM-1 expression induced by TNF-α more strongly than that induced by IL-1α in human lung carcinoma A549 cells. Mycotrienin II was found to inhibit protein synthesis in intact living cells, as well as in cell-free translation systems. Among translation inhibitors tested, acetoxycycloheximide and anisomycin, but neither puromycin nor emetine, inhibited the TNF-α-induced ICAM-1 expression at lower concentrations than the IL-1α-induced ICAM-1 expression. Several compounds of the triene-ansamycin group (that is, mycotrienin I, trienomycin A, trierixin, quinotrierixin and quinotrierixin HQ) also inhibited ICAM-1 expression, as well as cell-free translation in a manner similar to mycotrienin II. These results indicate that mycotrienin II is a direct inhibitor of translation, thereby inhibiting ICAM-1 expression induced by pro-inflammatory cytokines.
The Journal of Antibiotics (2011) **64**, 361–366; doi:10.1038/ja.2011.23; published online 30 March 2011

Keywords: ICAM-1; IL-1α; mycotrienin II; NF-κB; pro-inflammatory cytokine; TNF-α; triene-ansamycin

INTRODUCTION

Pro-inflammatory cytokines, such as tumor necrosis factor (TNF)-α and interleukin-1α (IL-1α), induce the expression of a variety of genes essential for inflammatory responses, such as intercellular adhesion molecule-1 (ICAM-1; CD54).[1] ICAM-1 is a cell-surface glycoprotein that binds to lymphocyte function-associated antigen-1 (CD11a/CD18) and Mac-1 (CD11b/CD18).[2] As one of its physiological roles, ICAM-1 inducibly expressed on vascular endothelial cells is required for the recruitment of leukocytes via the interaction with lymphocyte function-associated antigen-1 or Mac-1 and their subsequent transmigration to inflamed sites.[3,4] ICAM-1 expression is known to be induced primarily by the transcription factor nuclear factor-κB.[1] So far, many small molecules targeting the nuclear factor-κB signaling pathway induced by pro-inflammatory cytokines have been identified.[5]

Mycotrienin II (Figure 1a) was isolated from *Streptomyces* sp. and belongs to the triene-ansamycin group of compounds.[6,7] Mycotrienin II possesses various biological activities in mammalian cells, such as cytotoxicity and inhibition of osteoclastic bone resorption and endoplasmic reticulum (ER) stress-induced X-box binding protein 1 activation.[8–13] In the course of our screening for anti-inflammatory agents, we found that mycotrienin II inhibits ICAM-1 expression induced by TNF-α and IL-1α. In this study, we further investigated the molecular mechanism underlying the inhibition of ICAM-1 expression by mycotrienin II.

MATERIALS AND METHODS

Cell culture

Human lung carcinoma A549 cells were provided by the Health Science Research Resources Bank (Tokyo, Japan). A549 cells were maintained in RPMI 1640 medium (Invitrogen, Carlsbad, CA, USA) supplemented with 10% (v/v) heat-inactivated fetal calf serum (JRH Biosciences, Lenexa, KS, USA) and penicillin-streptomycin mixed solution (Nacalai Tesque, Kyoto, Japan).

Reagents

Recombinant human TNF-α and human IL-1α were kindly provided by Dainippon Pharmaceutical (Osaka, Japan). Mycotrienin I, mycotrienin II, trienomycin A, trierixin and quinotrierixin were isolated from the culture broth of *Streptomyces* sp. PAE37.[13] Quinotrierixin HQ, 13–ketomycotrienin I and 13–ketomycotrienin II were prepared as described previously.[13] Acetoxycycloheximide was isolated from the culture broth of an unidentified actinomycete strain designated by ML44-113F2.[14] Anisomycin and cycloheximide were purchased from Wako Pure Chemical Industries (Osaka, Japan). Emetine and puromycin were obtained from Sigma-Aldrich (St Louis, MO, USA).

[1]Department of Applied Biology, Kyoto Institute of Technology, Matsugasaki, Sakyo-ku, Kyoto, Japan and [2]Department of Biosciences and Informatics, Faculty of Science and Technology, Keio University, Yokohama, Japan
Correspondence: Dr T Kataoka, Department of Applied Biology, Kyoto Institute of Technology, Matsugasaki, Kyoto 606-8585, Japan.
E-mail: takao.kataoka@kit.ac.jp
Received 3 December 2010; revised 14 February 2011; accepted 17 February 2011; published online 30 March 2011

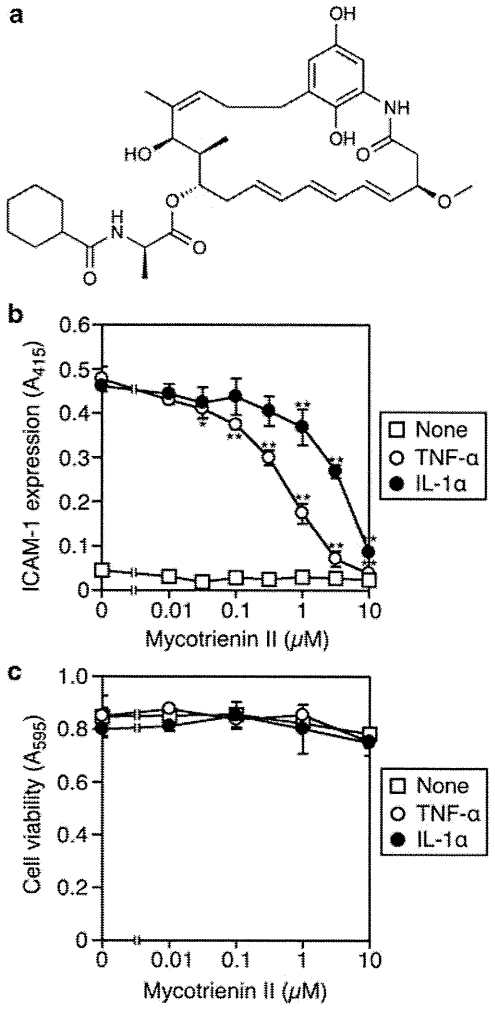

Figure 1 Mycotrienin II inhibits cell-surface intercellular adhesion molecule-1 (ICAM-1) expression induced by tumor necrosis factor-α (TNF-α) and interleukin-1α (IL-1α). (**a**) Structure of mycotrienin II. (**b**) A549 cells were pretreated with various concentrations of mycotrienin II for 1 h and then incubated with TNF-α (2.5 ng ml^{-1}; open circles) or IL-1α (0.25 ng ml^{-1}; filled circles) or without cytokines (open squares) for 6 h in the presence of mycotrienin II. ICAM-1 expression (A_{415}) is shown as means ± s.d. (n=3). *P<0.05 and **P<0.01, compared with control. Data are representative of two independent experiments. (**c**) A549 cells were incubated with various concentrations of mycotrienin II for 1 h and then incubated with TNF-α (2.5 ng ml^{-1}; open circles) or IL-1α (0.25 ng ml^{-1}; filled circles) or without cytokines (open squares) for 6 h in the presence of mycotrienin II. Cell viability (A_{595}) is shown as means ± s.d. (n=3). *P<0.05 and **P<0.01, compared with control. Data are representative of two independent experiments.

Assay for cell-surface expression of ICAM-1

A549 cells were washed twice with phosphate-buffered saline (PBS) and fixed with 1% paraformaldehyde–PBS for 15 min. After washing twice with PBS, the cells were incubated with 1% bovine serum albumin (Sigma-Aldrich)–PBS overnight. Fixed cells were treated with mouse anti-human ICAM-1 IgG antibody (clone 15.2; Leinco Technologies, St Louis, MO, USA) for 60 min and then washed three times with 0.02% Tween 20–PBS. The cells were further treated with horseradish peroxidase-linked anti-mouse IgG antibody (Jackson Immunoresearch, West Grove, PA, USA) for 60 min and then washed three times with 0.02% Tween-20–PBS. To develop the colorimetric reaction, the cells were incubated with the substrate solution (0.2 M sodium citrate (pH 5.3), 0.1% *o*-phenylenediamine dihydrochloride, 0.02% H_2O_2) for 20 min at 37 °C. Absorbance at 415 nm was measured with a Model 680 microplate reader (Bio-Rad Laboratories, Hercules, CA, USA).

Assay for cell viability

A549 cells were pulsed with MTT (3-(4,5-dimethylthiazol-2-yl)-2,5-diphenyltetrazolium bromide, 500 μg ml^{-1}) for 4 h and resultant MTT formazan was solubilized with 5% sodium dodecyl sulfate overnight. Absorbance at 595 nm was measured with a Model 680 microplate reader (Bio-Rad Laboratories).

Assay for macromolecular synthesis

A549 cells were pulse-labeled with [4,5-^{3}H]L-leucine (41.66 TBq mmol^{-1}; Moravek Biochemicals, Brea, CA, USA), [methyl-^{3}H]thymidine (2.37 TBq mmol^{-1}; MP Biomedicals, Santa Ana, CA, USA), and [5-^{3}H]uridine (0.626 TBq mmol^{-1}; Moravek Biomedicals) for the indicated times. The labeled cells were washed three times with PBS and then lysed with 250 mM NaOH for 15 min, followed by 1 h incubation on ice in the presence of 5% trichloroacetic acid. The precipitates and the supernatants were separated by centrifugation (10 000×*g*, 5 min). Radioactivity was measured with a 1900CA TRI-CARB liquid scintillation analyzer (Packard Instrument, Meriden, CT, USA).

Assay for cell-free protein synthesis

The T7-driven luciferase cDNA was subjected to the cell-free reaction (30 °C, 90 min) for transcription and translation by the TnT T7 Coupled Reticulocyte Lysate Systems (Promega, Madison, WI, USA). Luciferase mRNA was subjected to the cell-free reaction (30 °C, 90 min) for translation by the Rabbit Reticulocyte Lysate System (Promega). Reaction mixtures were mixed with the luciferase assay solution and relative light units were immediately measured with a Lumitester K-100 Luminometer (Hamamatsu Photonics, Hamamatsu, Japan).

Statistical analysis

Statistical significance was assessed by one-way analysis of variance, followed by the Tuker test for multiple comparisons using KaleidaGraph (Synergy Software, Reading, PA, USA). Differences of P<0.05 were considered to be statistically significant.

RESULTS

Mycotrienin II inhibits cell-surface ICAM-1 expression induced by TNF-α and IL-1α

Pro-inflammatory cytokines, such as TNF-α or IL-1α, induce the expression of various cell-surface molecules during inflammatory responses.[1] Upon stimulation with TNF-α or IL-1α, lung carcinoma A549 cells expressed ICAM-1 on their cell surface. Mycotrienin II was found to inhibit the cell-surface ICAM-1 expression induced by TNF-α and IL-1α in a dose-dependent manner (Figure 1b). As its characteristic inhibitory profiles, the TNF-α-induced ICAM-1 expression (IC_{50} value: 0.3 μM) was more strongly inhibited by mycotrienin II than the IL-1α-induced ICAM-1 expression (IC_{50} value: 3.1 μM). During the same incubation time, mycotrienin II exerted a marginal effect on cell viability up to 10 μM even in the presence of TNF-α or IL-1α (Figure 1c). Consistent with these data, mycotrienin II did not induce the release of L-lactose dehydrogenase into the culture medium in the presence or absence of TNF-α or IL-1α (data not shown). These results indicate that the inhibition of cell-surface ICAM-1 expression by mycotrienin II is not likely to be nonspecific cytotoxicity and induction of cell death.

Mycotrienin II inhibits cellular and cell-free translation

Recently, it has been shown by us and other group that the trine-ansamycin group compounds, such as cytotrienin A and quinotrierixin, are translation inhibitors.[15,16] To investigate whether mycotrienin

II selectively affects *de novo* protein synthesis at the cellular level, A549 cells were pretreated with mycotrienin II and then pulse-labeled with [^{3}H]L-leucine, [^{3}H]thymidine, and [^{3}H]uridine in the presence of the compound. Then, the amount of radioactivity incorporated into the acid-insoluble (macromolecular) fractions was measured. Mycotrienin II inhibited the incorporation of [^{3}H]L-leucine in a dose-dependent manner and at the IC_{50} value of 0.058 μM (Figure 2a), whereas mycotriein II did not obviously affect the incorporation of [^{3}H]thymidine and [^{3}H]uridine (Figure 2b). When [^{3}H]L-leucine-labeled cell lysates were separated into acid-soluble supernatants and acid-insoluble precipitates, mycotrienin II inhibited the incorporation of radioactivity into the precipitates, but conversely increased the radioactivity incorporation into the supernatants (Figure 2c). Thus, these results suggest that mycotrienin II does not affect the uptake of amino acids across the plasma membrane, but directly prevents translation.

To further investigate whether mycotrienin II directly affects translation, luciferase cDNA or luciferase mRNA was used as a template for transcription and translation in cell-free systems, based on rabbit reticulocyte lysates. The resultant luciferase activity associated with the protein products was measured. Mycotrienin II suppressed the luciferase activity in the cell-free transcription-coupled translation system (IC_{50} value: 5.5 μM) (Figure 2d) and the cell-free translation system (IC_{50} value: 4.1 μM) (Table 1) at equivalent concentrations. These results indicate that mycotrienin II directly prevents translation.

The triene-ansamycin group of compounds inhibits TNF-α/IL-1α-induced ICAM-1 expression and translation

To obtain additional evidence that the inhibition of ICAM-1 expression by mycotrienin II is primarily caused by the prevention of translation, the structure-activity relationship of the triene-ansamycin group of compounds (Figure 3) was investigated. In the inhibitory profiles similar to that of mycotrienin II (Figure 1b), mycotrienin I, trienomycin A, trierixin, quinotrierixin and quinotrierixin HQ inhibited the TNF-α-induced ICAM-1 expression more preferentially than the IL-1α-induced ICAM-1 expression, whereas 13-ketomycotrienin I, 13-ketomycotrienin II and demethyltrienomycinol were totally inactive up to 10 μM (Table 1). Consistent with these data, mycotrienin I, trienomycin A, trierixin, quinotrierixin and quinotrierixin HQ

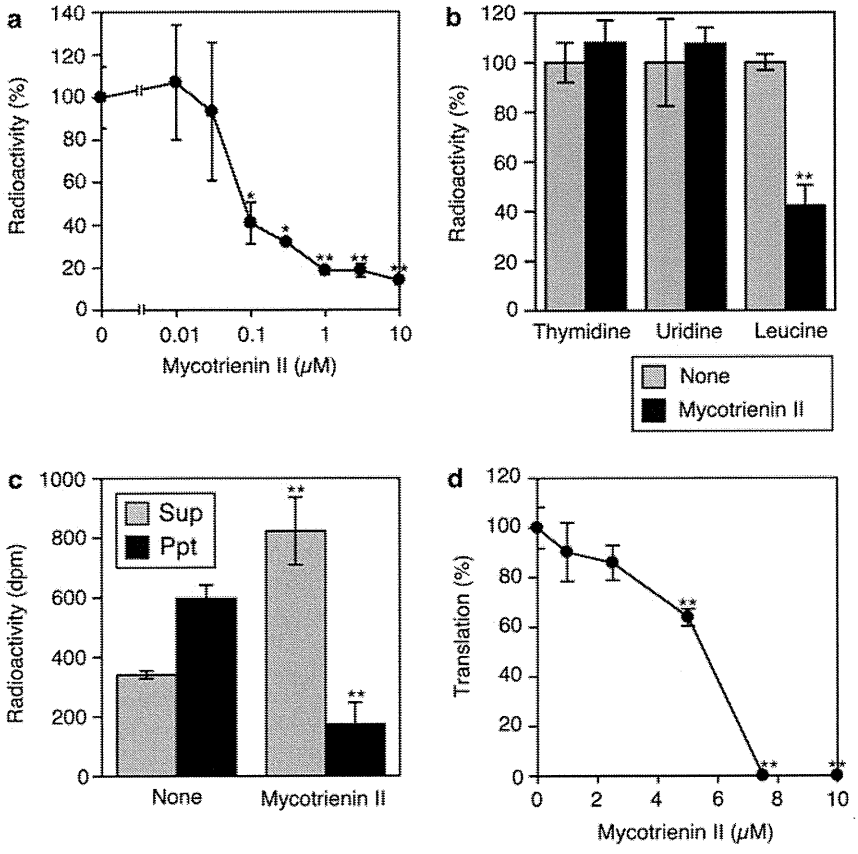

Figure 2 Mycotrienin II directly inhibits *de novo* protein synthesis. (**a**) A549 cells were pretreated with various concentrations of mycotrienin II for 1 h and pulse-labeled with [^{3}H]L-leucine for 2 h in the presence or absence of mycotrienin II. Radioactivity incorporated into the acid-insoluble fractions was measured. Radioactivity (%) is shown as means ± s.d. (n=3). *P<0.05 and **P<0.01, compared with control. Data are representative of two independent experiments. (**b**) A549 cells were pretreated with (black bars) or without (gray bars) mycotrienin II (1 μM) for 30 min and then pulse-labeled with [^{3}H]thymidine, [^{3}H]uridine or [^{3}H]L-leucine for 1 h in the presence or absence of mycotrienin II. Radioactivity incorporated into the acid-insoluble fractions was measured. Radioactivity (%) is shown as means ± s.d. (n=3). *P<0.05 and **P<0.01, compared with control. Data are representative of two independent experiments. (**c**) A549 cells were pretreated with or without mycotrienin II (1 μM) for 1 h and then pulse-labeled with [^{3}H]L-leucine for 2 h in the presence or absence of mycotrienin II. Acid-soluble fractions as supernatants (Sup; gray bars) and acid-insoluble fractions as precipitates (Ppt; filled bars) were collected and measured for radioactivity. Radioactivity (dpm) is shown as means ± s.d. (n=3). *P<0.05 and **P<0.01, compared with control. Data are representative of two independent experiments. (**d**) Luciferase cDNA was transcribed and then translated by rabbit reticulocyte lysates in the presence of various concentrations of mycotrienin II. Luciferase activity (%) is shown as means ± s.d. (n=3). *P<0.05 and **P<0.01, compared with control. Data are representative of two independent experiments.

inhibited the cell-free translation at comparable concentrations, whereas 13-ketomycotrienin I, 13-ketomycotrienin II and demethyltrienomycinol were inert up to 10 μM (Table 1). These results indicate that the inhibition of ICAM-1 expression by the triene-ansamycin group of compounds is closely related to their ability to prevent translation.

Effect of translation inhibitors on ICAM-1 expression induced by TNF-α and IL-1α

The above observation that the triene-ansamycin group compounds inhibited the TNF-α-induced ICAM-1 expression more preferentially than the IL-1α-induced ICAM-1 expression prompted us to investigate the effect of other translation inhibitors on ICAM-1 expression induced by TNF-α and IL-1α. As reported in our previous paper,[14] acetoxycycloheximide inhibited the TNF-α-induced ICAM-1 expression at much lower concentrations than the IL-1α-induced ICAM-1 expression (Figure 4a), whereas cycloheximide prevented the TNF-α- and IL-1α-induced ICAM-1 expression at relatively similar concentrations (Figure 4b). By contrast, anisomycin inhibited the TNF-α-induced ICAM-1 expression more strongly than the IL-1α-induced ICAM-1 expression (Figure 4c), whereas puromycin and emetine prevented the TNF-α- and IL-1α-induced ICAM-1 expression at equivalent concentrations (Figures 4d and e). These data indicate that the triene-ansamycin group compounds exert inhibitory profiles similar to acetoxycycloheximide and anisomycin.

Table 1 Biological activities of triene-ansamycin group of compounds

	ICAM-1 expression[a]		
Compound	*TNF-α*	*IL-1α*	*Translation*[b]
Mycotrienin I	0.57	4.9	6.2
Mycotrienin II	0.3	3.1	4.1
Trienomycin A	0.61	3.0	4.4
13-Ketomycotrienin I	>10	>10	>10
13-Ketomycotrienin II	>10	>10	>10
Trierixin	0.16	0.62	2.2
Quinotrierixin	0.84	4.7	2.8
Quinotrierixin HQ	1.3	6.2	3.7
Demethyltrienomycinol	>10	>10	>10

Abbreviations: ICAM-1, intercellular adhesion molecule-1; IL-1α, interleukin-1α; TNF-α, tumor necrosis factor-α.
[a]A549 cells were preincubated with serial dilutions of compounds for 1 h and then incubated with TNF-α (2.5 ng ml^{-1}) or IL-1α (0.25 ng ml^{-1}) for 6 h in the presence or absence of compounds. ICAM-1 expression (%) was determined by triplicate cultures. The means of IC_{50} values (μM) were calculated from three independent experiments.
[b]Luciferase mRNA was translated by rabbit reticulocyte lysates in the presence of serial dilutions of compounds at 30 °C for 90 min. Luciferase activity (%) was determined by triplicate measurements. The means of IC_{50} values (μM) were calculated from two independent experiments, except for trierixin.

DISCUSSION

Cytotrienin A, a structural derivative of mycotrienin II, was initially identified as an inducer of apoptosis.[17,18] Recently, it has been shown that cytotrienin A inhibits eukaryotic protein synthesis by targeting translation elongation and interfering with eukaryotic elongation factor 1A function.[15] Consistent with this and our findings,[15,16] mycotrienin II and its structural derivatives inhibited cellular protein synthesis and cell-free translation. Nevertheless, the *de novo* protein synthesis in intact living cells (Figure 2a) was inhibited much more strongly by mycotrienin II than the cell-free translation (Table 1). The difference in sensitivity is in agreement with the observation that cytotrienin A inhibits cellular protein synthesis more strongly than the cell-free translation.[15] This may be because the cell-free translation systems contain larger amounts of proteins that bind to mycotrienin II or cytotrienin A (most likely eukaryotic elongation factor 1A) than living cells, and therefore higher concentrations of the compounds are required for the inhibition of translation.

Nevertheless, the concentrations of mycotrienin II required to inhibit the IL-1α-induced ICAM-1 expression (Figures 1b) were still higher than those required to inhibit constitutive *de novo* protein synthesis monitored by [^{3}H]L-leucine incorporation (Figure 2a). By contrast, we have shown that the protein synthesis inhibitor cycloheximide prevents cellular protein synthesis and IL-1α-induced ICAM-1 expression at

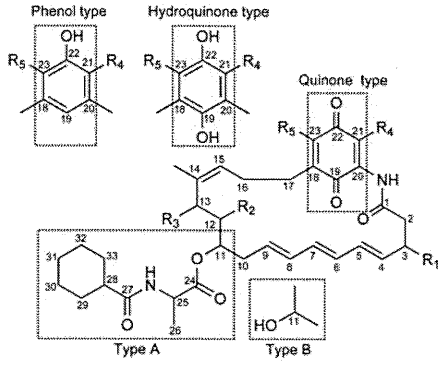

Compound	Structural unit	R_1	R_2	R_3	R_4	R_5	Side chain
Mycotrienin I	Quinone	OCH_3	CH_3	OH	H	H	A
Mycotrienin II	Hydroquinone	OCH_3	CH_3	OH	H	H	A
Trienomycin A	Phenol	OCH_3	CH_3	OH	H	H	A
13-ketomycotrienin I	Quinone	OCH_3	CH_3	=O	H	H	A
13-Ketomycotrienin II	Hydroquinone	OCH_3	CH_3	=O	H	H	A
Trierixin	Hydroquinone	OCH_3	CH_3	OH	SCH_3	H	A
Quinotrierixin	Quinone	OCH_3	CH_3	OH	H	SCH_3	A
Quinotrierixin HQ	Hydroquinone	OCH_3	CH_3	OH	H	SCH_3	A
Demetyltrienomycinol	Phenol	OH	H	OH	H	H	B

Figure 3 Structures of triene-ansamycin groups of compounds.

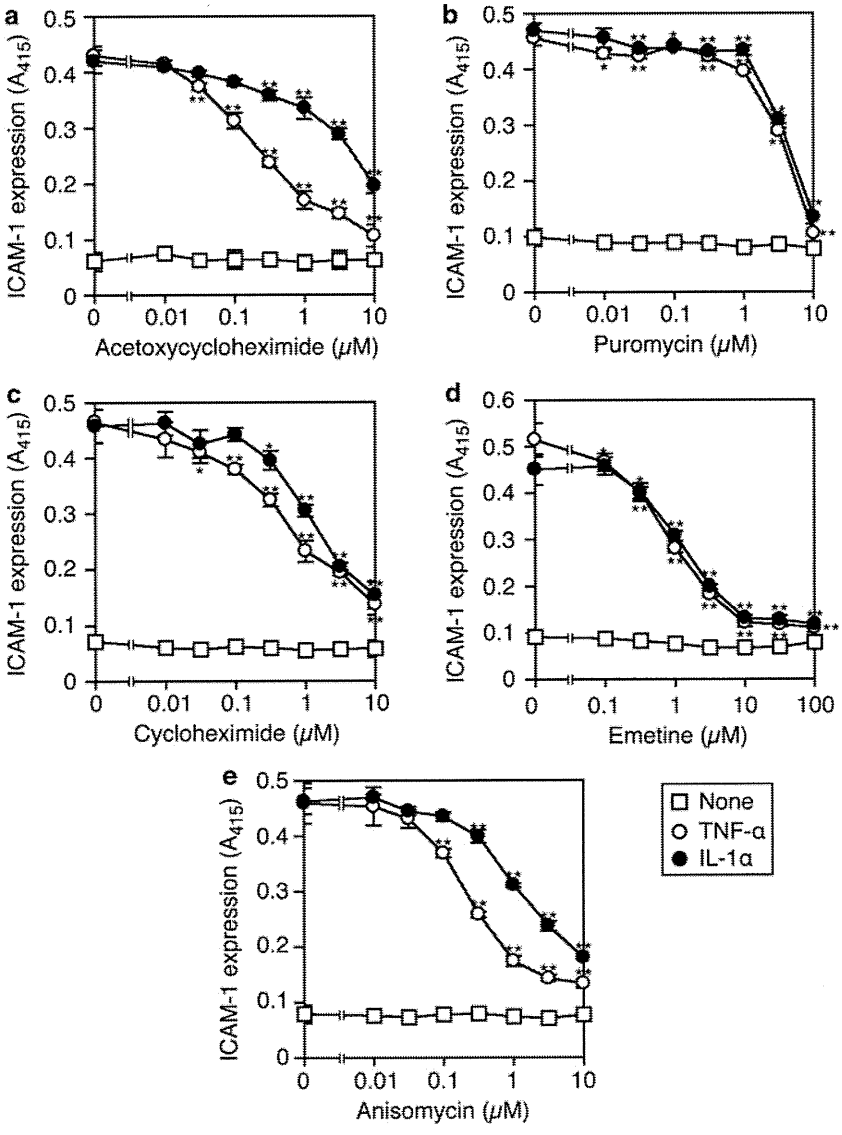

Figure 4 Effect of translation inhibitors on cell-surface intercellular adhesion molecule-1 (ICAM-1) expression induced by tumor necrosis factor-α (TNF-α) and interleukin-1α (IL-1α). A549 cells were pretreated with various concentrations of acetoxycycloheximide (**a**), cycloheximide (**b**), anisomycin (**c**), puromycin (**d**) or emetine (**e**) for 1 h and then incubated with TNF-α (2.5 ng ml^{-1}; open circles) or IL-1α (0.25 ng ml^{-1}; filled circles) or without cytokines (open squares) for 6 h in the presence of the compound. ICAM-1 expression (A_{415}) is shown as means ± s.d. (n=3). *P<0.05 and **P<0.01, compared with control. Data are representative of two independent experiments.

relatively similar concentrations in A549 cells.[14] Eukaryotic elongation factor 1A is indispensable for the translation of all polypeptide-encoded mRNAs in that it has an essential role in the delivery of the aminoacyl-tRNA to the ribosome A site and the subsequent GTP hydrolysis. Therefore, the inhibitory effect of mycotrienin II may be influenced by unidentified intracellular factors and/or conditions other than eukaryotic elongation factor 1A in intact living cells.

The present structure-activity relationship study demonstrated that the hydroxyl group at C-13 is essential for the inhibitory activities of the triene-ansamycin compounds on ICAM-1 expression, as well as the cell-free translation, whereas the difference in the benzenoid moiety (phenol, hydroquinone and quinone) did not alter the inhibitory activities (Table 1). These properties of the triene-ansamycin group are in agreement with the structure-activity relationship study of the inhibitors of endoplasmic reticulum stress-induced X-box binding protein 1 activation.[13] In addition, mycotrienin II and its five structural derivatives inhibited the TNF-α-induced ICAM-1 expression several times more strongly than the IL-1α-induced ICAM-1 expression (Table 1). As shown in Figure 3, these characteristic inhibitory profiles were observed with translation inhibitors that potently induce ribotoxic stress response (acetocycloheximide and anisomycin), but not obviously observed with those that induce ribotoxic stress response weakly or not at all (cycloheximide, puromycin and emetine).[19–23] Ribotoxic stress response caused by translation inhibitors triggers the activation of the mitogen-activated protein kinase superfamily, thereby leading to diverse cellular responses, such as gene expression and apoptosis.[19–26]

Ectodomain shedding is a critical posttranslational mechanism for the regulation of the function of membrane-anchored ligands and receptors. TNF-α-converting enzyme cleaves many transmembrane proteins, including TNF-α and TNF receptor 1 (TNF-R1), into their soluble forms and has a regulatory role in TNF-α-dependent cellular

responses.[27,28] We have previously shown that acetoxycycloheximide induces the ectodomain shedding of TNF-R1 by TNF-α-converting enzyme in a manner that is dependent on the activation of extracellular-signal regulated kinase and p38 mitogen-activated protein kinase in A549 cells.[22,23] Consistently, we observed that mycotrienin II induced the upregulation of soluble extracellular TNF-R1 in A549 cells and that it was prevented by the TNF-α-converting enzyme inhibitor TAPI-2 (unpublished data). Thus, mycotrienin II seems to induce the ectodomain shedding of TNF-R1 in a manner similar to acetoxycycloheximide. Because the ectodomain shedding of TNF-R1 by TNF-α-converting enzyme weakens responsiveness to TNF-α, it seems possible that mycotrienin II is able to trigger activation of the mitogen-activated protein kinase superfamily and thereby induce the ectodomain shedding of TNF-R1, leading to the reduction of TNF-α responsiveness. Ribotoxic stress response possibly induced by the triene-ansamycin group compounds may account for the preferential inhibition of the TNF-α-induced ICAM-1 expression rather than the IL-1α-induced ICAM-1 expression.

ACKNOWLEDGEMENTS

We are very grateful to Drs. Kazuo Nagai, Yoshinori Tsukumo and Rei Koyanagi for their initial contributions to start this work. This work was supported by a Grant-in-Aid for Scientific Research (KAKENHI) from Japan Society for the Promotion of Science (JSPS) and a Grant-in-Aid from the Naito Foundation.

1 Collins, T. *et al.* Transcriptional regulation of endothelial cell adhesion molecules: NF-κB and cytokine-inducible enhancers. *FASEB J.* **9,** 899–909 (1995).
2 Springer, T. A. Adhesion receptors of the immune system. *Nature* **346,** 425–434 (1990).
3 Springer, T. A. Traffic signals for lymphocyte recirculation and leukocyte emigration: the multistep paradigm. *Cell* **76,** 301–314 (1994).
4 Cook-Mills, J. M. & Deem, T. L. Active participation of endothelial cells in inflammation. *J. Leukoc. Biol.* **77,** 487–495 (2005).
5 Kataoka, T. Chemical biology of inflammatory cytokine signaling. *J. Antibiot.* **62,** 655–667 (2009).
6 Coronelli, C., Pasqualucci, R. C., Thiemann, J. E. & Tamoni, G. Mycotrienin, a new polyene antibiotic isolated from Streptomyces. *J. Antibiot.* **20,** 329–333 (1967).
7 Sugita, M., Sasaki, T., Furihata, K., Seto, H. & Otake, N. Studies on mycotrienin antibiotics, a novel class of ansamycins. II. Structure elucidation and biosynthesis of mycotrienins I and II. *J. Antibiot.* **35,** 1467–1473 (1982).
8 Sugita, M. *et al.* Studies on mycotrienin antibiotics, a novel class of ansamycins. I. Taxonomy, fermentation, isolation and properties of mycotrienin I and II. *J. Antibiot.* **35,** 1460–1466 (1982).
9 Sugita, M. *et al.* Studies on mycotrienin antibiotics, a novel class of ansamycins. III. The isolation, characterization and structures of mycotrienols I and II. *J. Antibiot.* **35,** 1474–1479 (1982).
10 Sugita, M. *et al.* Studies on mycotrienin antibiotics, a novel class of ansamycins. IV. Microbial conversion of mycotrienin-II to mycotrienol-II, 34-hydroxymycotrienin-II and 22-*O*-β-D-glucopyranosyl mycotrienin-II by *Bacillus megaterium*. *J. Antibiot.* **38,** 799–802 (1985).
11 Feuerbach, D., Waelchli, R., Fehr, T. & Feyen, J. H. M. Mycotrienins. A new class of potent inhibitors of osteoclastic bone resorption. *J. Biol. Chem.* **270,** 25949–25955 (1995).
12 Tashiro, E. *et al.* Trierixin, a novel inhibitor of ER stress-induced XBP1 activation from *Streptomyces* sp. I. Taxonomy, fermentation, isolation, and biological activities. *J. Antibiot.* **60,** 547–553 (2007).
13 Kawamura, T., Tashiro, E., Yamamoto, K., Shindo, K. & Imoto, M. SAR study of a novel triene-ansamycin group compound, quinotrierixin, and related compounds, as inhibitors of ER stress-induced XBP1 activation. *J. Antibiot.* **61,** 303–311 (2008).
14 Sugimoto, H. *et al.* E-73, an acetoxyl analogue of cycloheximide, blocks the tumor necrosis factor-induced NF-κB signaling pathway. *Biochem. Biophys. Res. Commun.* **277,** 330–333 (2000).
15 Lindqvist, L. *et al.* Inhibition of translation by cytotrienin A–a member of the ansamycin family. *RNA* **16,** 2404–2413 (2010).
16 Yamamoto, K., Tashiro, E. & Imoto, M. Quinotrierixin inhibits ER stress-induced XBP1 mRNA splicing through inhibition of protein synthesis. *Biosci. Biotechnol. Biochem.* **75,** 284–288 (2011).
17 Kakeya, H. *et al.* Cytotrienin A, a novel apoptosis inducer in human leukemia HL-60 cells. *J. Antibiot.* **50,** 370–372 (1997).
18 Zhang, H. P., Kakeya, H. & Osada, H. Novel triene-ansamycins, cytotrienins A and B, inducing apoptosis on human leukemia HL-60. *Tetrahedron Lett.* **38,** 1789–1792 (1997).
19 Iordanov, M. S. *et al.* Ribotoxic stress response: activation of the stress-activated protein kinase JNK1 by inhibitors of the peptidyl transferase reaction and by sequence-specific RNA damage to the α-sarcin/ricin loop in the 28S rRNA. *Mol. Cell. Biol.* **17,** 3373–3381 (1997).
20 Sidhu, J. S. & Omiecinski, C. J. Protein synthesis inhibitors exhibit a nonspecific effect on phenobarbital-inducible cytochome P450 gene expression in primary rat hepatocytes. *J. Biol. Chem.* **273,** 4769–4775 (1998).
21 Shifrin, V. I. & Anderson, P. Trichothecene mycotoxins trigger a ribotoxic stress response that activates c-Jun N-terminal kinase and p38 mitogen-activated protein kinase and induces apoptosis. *J. Biol. Chem.* **274,** 13985–13992 (1999).
22 Ogura, H. *et al.* Ectodomain shedding of TNF receptor 1 induced by protein synthesis inhibitors regulates TNF-α-mediated activation of NF-κB and caspase-8. *Exp. Cell Res.* **314,** 1406–1414 (2008).
23 Ogura, H. *et al.* ERK and p38 MAP kinase are involved in downregulation of cell surface TNF receptor 1 induced by acetoxycycloheximide. *Inter. Immunopharmacol.* **8,** 922–926 (2008).
24 Kadohara, K. *et al.* Acetoxycycloheximide (E-73) rapidly induces apoptosis mediated by the release of cytochrome *c* via activation of c-Jun N-terminal kinase. *Biochem. Pharmacol.* **69,** 551–560 (2005).
25 Kadohara, K. *et al.* Caspase-8 mediates mitochondrial release of pro-apoptotic proteins in a manner independent of its proteolytic activity in apoptosis induced by the protein synthesis inhibitor acetoxycycloheximide in human leukemia Jurkat cells. *J. Biol. Chem.* **284,** 5478–5487 (2009).
26 Chinen, T. *et al.* Irciniastatin A induces JNK activation that is involved in caspase-8-dependent apoptosis via the mitochondrial pathway. *Toxicol. Lett.* **199,** 341–346 (2010).
27 Schlöndorff, J. & Blobel, C. P. Metalloprotease-disintegrins: modular proteins capable of promoting cell-cell interactions and triggering signals by protein-ectodomain shedding. *J. Cell Sci.* **112,** 3603–3617 (1999).
28 Moss, M. L., White, J. M., Lambert, M. H. & Andrews, R. C TACE and other ADAM proteases as targets for drug discovery. *Drug Discov. Today* **6,** 417–426 (2001).

Bioorganic & Medicinal Chemistry 19 (2011) 4377–4385

Contents lists available at ScienceDirect

Bioorganic & Medicinal Chemistry

journal homepage: www.elsevier.com/locate/bmc

Generation of 'Unnatural Natural Product' library and identification of a small molecule inhibitor of XIAP

Tatsuro Kawamura [a], Kohei Matsubara [a], Hitomi Otaka [a], Etsu Tashiro [a], Kazutoshi Shindo [b], Ryo C. Yanagita [c], Kazuhiro Irie [c], Masaya Imoto [a,*]

[a] Department of Biosciences and Informatics, Faculty of Science and Technology, Keio University, 3-14-1 Hiyoshi, Kohoku-ku, Yokohama 223-8522, Japan
[b] Department of Food and Nutrition, Japan Women's University, 2-8-1, Mejirodai, Bunkyo-ku, Tokyo 112-8681, Japan
[c] Division of Food Science and Biotechnology, Graduate School of Agriculture, Kyoto University, Kyoto 606-8502, Japan

ARTICLE INFO

Article history:
Received 8 April 2011
Revised 10 May 2011
Accepted 10 May 2011
Available online 27 May 2011

Keywords:
Chemical library
Natural product
Unnatural Natural Product
C38OX6
XIAP
Cancer

ABSTRACT

Natural products have been utilized for drug discovery. To increase the source diversity, we generated a new chemical library consisting of chemically modified microbial metabolites termed 'Unnatural Natural Products' by chemical conversion of microbial metabolites in crude broth extracts followed by purification of reaction products with the LC-photo diode array–MS system. Using this library, we discovered an XIAP inhibitor, C38OX6, which restored XIAP-suppressed enzymatic activity of caspase-3 in vitro. Furthermore, C38OX6 sensitized cancer cells to anticancer drugs, whereas the unconverted natural product did not. These findings suggest that our library could be a useful source for drug seeds.

1. Introduction

It is now recognized that evasion of apoptosis is a hallmark of human cancer. One cause of resistance to apoptosis is overexpression of anti-apoptotic proteins, including inhibitor of apoptosis (IAP) family proteins. X-linked inhibitor of apoptosis (XIAP) is a member of IAP family proteins, and overexpression of XIAP is often reported in several types of human cancer, such as acute myeloid leukemia (AML) and pancreatic cancer.[1] XIAP is an endogenous direct inhibitor of caspase-3, -7, and -9, which are key apoptosis signal mediators. In the structure of XIAP, three baculovirus IAP repeat (BIR) domains are conserved in IAP family proteins. The BIR2 domain with its flanking region of XIAP binds and inhibits active caspase-3/-7, whereas the BIR3 domain binds and inhibits caspase-9.[2–4] By inhibiting the enzymatic activities of these effector and initiator caspases, XIAP maintains cancer cell survival and renders cells resistant to apoptosis induction by radiation and anticancer drugs. Although XIAP is expressed in some normal tissues, no overt phenotype was detected in XIAP-deficient mice,[5] indicating that XIAP would be a promising molecular target for cancer therapies; therefore, we searched for compounds that inhibited XIAP function.

Traditionally, natural products have been a major source of lead molecules in drug development because natural products are highly diverse and often provide highly specific biological activities; however, obtaining drug-lead molecules from natural sources requires us to complete a series of time-consuming steps, including screening of extract libraries, bioassay-guided isolation, structure elucidation, and subsequent production scale-up. Therefore, over the past decade, combinatorial chemistry has become the major source of lead molecules in drug discovery; however, despite the increased speed of synthesis, this changeover from traditional to combinatorial synthesis has not yielded any real increase in the number of lead optimization candidates or drugs.[6] This apparent lack of productivity may be explained by the structural differences between natural and combinatorial compounds in that combinatorial compounds are substantially less diverse than natural products from many viewpoints, such as the number of chiral centers, the prevalence of aromatic rings, the introduction of complex ring systems, and the degree of saturation of the molecule as well as the number and ratios of different heteroatoms. Indeed, in the chemical space, natural products occupied a wide region, and the distribution of natural products (but not combinatorial compounds) is quite similar to that of approved drugs.[7] Therefore, natural

Abbreviations: UNP, Unnatural Natural Product; PDA, photo diode array.

* Corresponding author.
E-mail address: imoto@bio.keio.ac.jp (M. Imoto).

0968-0896/$ - see front matter © 2011 Elsevier Ltd. All rights reserved.
doi:10.1016/j.bmc.2011.05.009

products have been, yet again, recognized to play a dominant role in the discovery of leads for the development of drugs for the treatment of human diseases, and several industrial and academic groups are using natural products to construct high-quality screening libraries.[8,9] Methods have been developed to generate large and diverse natural product libraries optimized for high-throughput screening and for a fast discovery process. Recently, we have also constructed a semi-natural product library whose components are chemically modified microbial metabolites which are referred to as 'Unnatural Natural Products (UNPs)'. Here we report the details of our new method to generate the UNP library and discovery of a new XIAP inhibitor.

2. Results

2.1. Generation of 'Unnatural Natural Product' library

To generate the 'Unnatural Natural Product (UNP)' library, we devised a series of unique procedures consisting of (i) preparation of actinomycetal fermentation broth extracts, (ii) chemical conversion of actinomycetal metabolites in crude broth extracts, (iii) detection of newly generated components which are referred to as UNPs, and (iv) isolation of UNPs by chromatography (Fig. 1A). In these procedures, chemical conversion of actinomycetal metabolites was the key step; therefore, we first examined the reaction

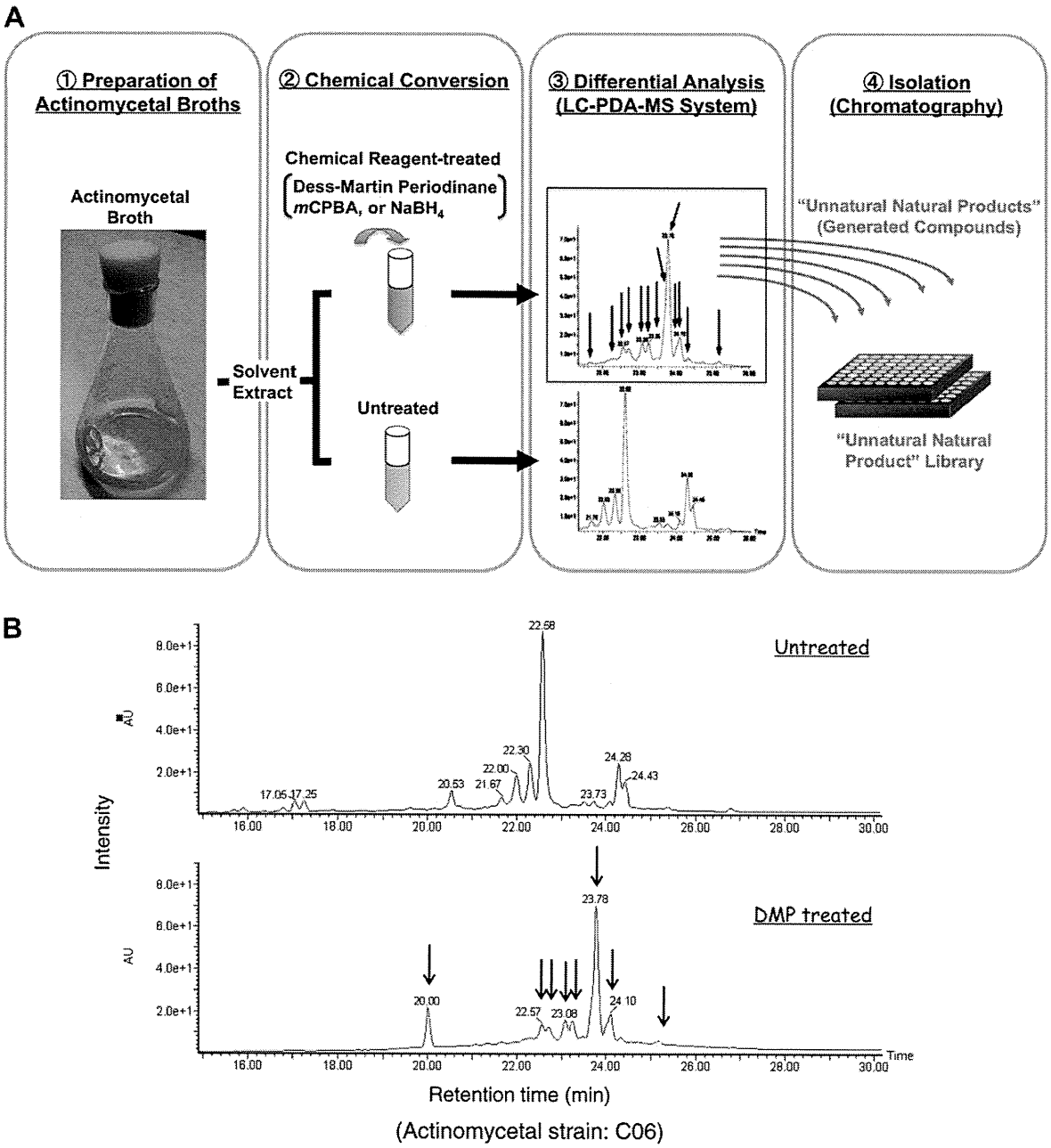

Figure 1. Generation of 'Unnatural Natural Product (UNP)' library. (A) Strategy for generation of UNP library. (B-D) Representative photo diode array (PDA) chromatogram of DMP, *m*CPBA or $NaBH_4$-treated or untreated actinomycetal broth extracts. Each actinomycetal broth extract was stirred with or without DMP in CH_2Cl_2 for 3 h (B), *m*CPBA in CH_2Cl_2 for 3 h (C), or $NaBH_4$ in MeOH for 1 h (D) at room temperature. Subsequently, the extracts of the reaction mixtures were analyzed by the LC–PDA–MS system (column: ODS, LC: 30–100% MeOH/H_2O (linear gradient) during 0–15 min and 100% MeOH during 15–45 min, detection: 220–600 nm). The peaks of UNPs were distinguished from those of unconverted natural products on the basis of their unique UV and MS spectra and retention time on HPLC. Representative peaks of UNPs are indicated with arrows.

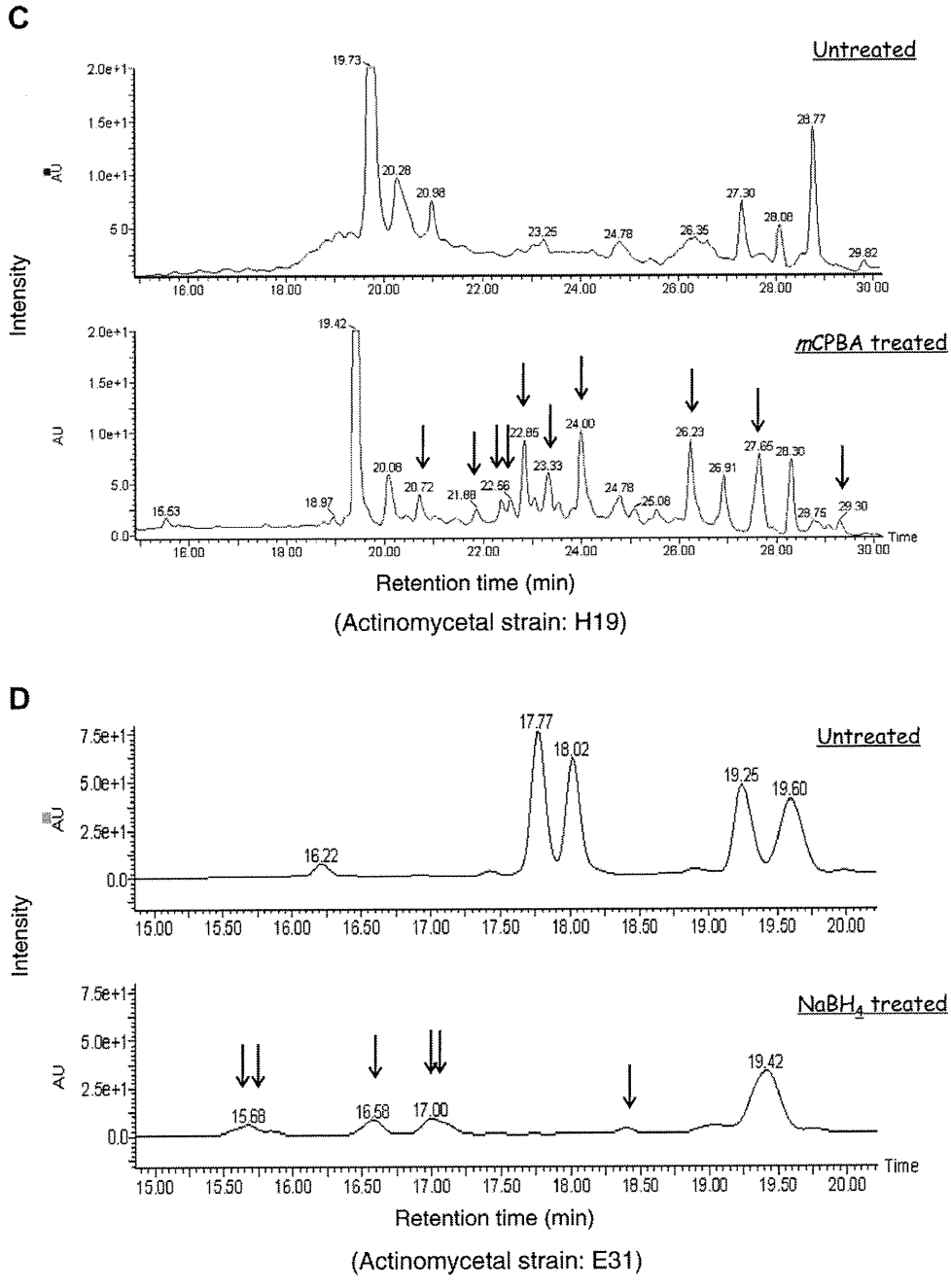

Fig. 1 (*continued*)

conditions, which efficiently converted diverse actinomycetal metabolites in the broth extracts without disruption of their natural product skeletons. As some natural products are unstable at extreme temperature and pH, we selected three types of relatively mild chemical reactions, oxidation by Dess–Martin periodinane (DMP), epoxidation by *meta*-chloroperbenzoic acid (*m*CPBA), and reduction by $NaBH_4$. Reaction products were separated through the HPLC unit, followed by spectral analyses in the detector units which gave us UV/vis and ESI-MS spectra (liquid chromatography-photo diode array–mass spectrometry (LC–PDA–MS) system), and distinguished from the unconverted actinomycetal metabolites (natural products). Each actinomycetal strain produces its own secondary metabolites with a huge variety of structures; therefore, by the addition of an equal weight of DMP or *m*CPBA to the actinomycetal broth extracts, many UNPs were produced through 3 h-chemical reaction at room temperature in many cases; however, the addition of excessive amounts of the chemical reagents caused the decomposition of UNPs. In a reduction reaction, chemical conversion was successful for 1 h by the addition of 10 times the amount of $NaBH_4$. Representative PDA chromatograms of the broth extracts with or without addition of chemical reagents are shown in Figure 1B–D. For the construction of the UNP library, UNPs in the reaction mixture were roughly purified by column chromatography on silica gel, and were further purified through the LC–PDA–MS system. The purity of isolated UNPs was also checked by the LC–PDA–MS system and the physico-chemical properties such as the retention times on the HPLC, UV/vis spectra, and ESI-MS spectra were stored to construct a database. Although the structure of each UNP in the library has not been elucidated, physico-chemical properties provide valuable structural information on each UNP.

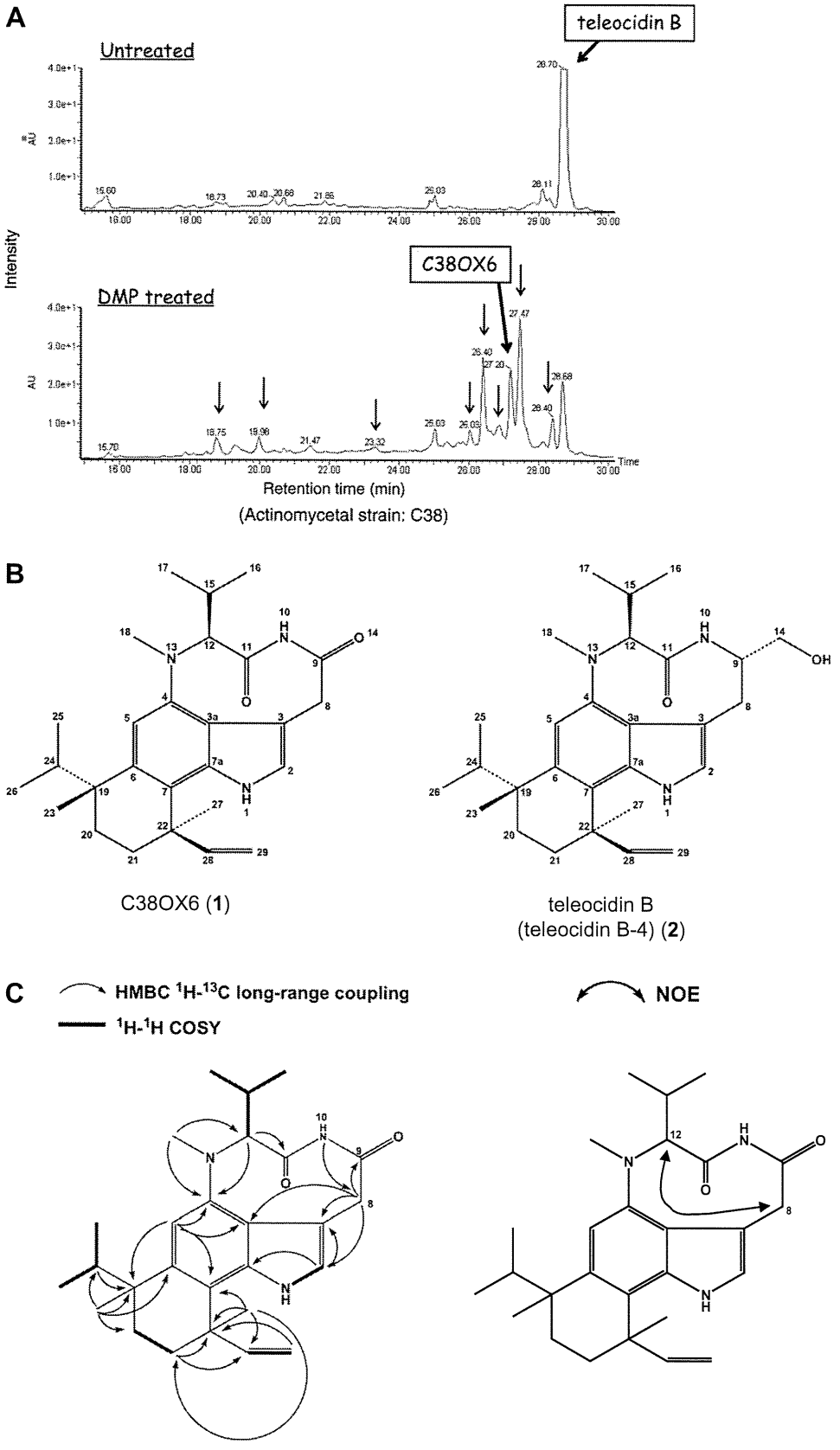

Figure 2. Structure elucidation of C38OX6 (**1**). (A) PDA chromatogram of DMP-treated or untreated broth extract of actinomycetal strain C38. Reaction and analysis conditions are as shown in Fig. 1B. Representative peaks of UNPs are indicated with arrows. (B) Structures of C38OX6 (**1**) and teleocidin B (**2**). (C) Structure elucidation of C38OX6 (**1**) by 2D-NMR spectroscopy.

2.2. Identification of C38OX6 (1) as XIAP inhibitor

Next, biological activities of each UNP were evaluated by several in-house assay systems. As a result, several UNPs showed biological activities such as apoptosis-inducing activity and migration inhibitory activity against cancer cells (data not shown). Among these active compounds, we focused on an UNP, C38OX6 (**1**), because it showed inhibitory activity against XIAP functions.

XIAP inhibits the enzymatic activity of caspase-3, resulting in cellular apoptosis suppression; therefore, to find candidate drug leads for tumor treatment, we searched for compounds in UNPs that could restore XIAP-suppressed caspase-3 activity. For this, we used the in vitro caspase de-repression assay using a fluorogenic peptide as a substrate.[10] As a result, one UNP, C38OX6, was found to overcome XIAP-mediated suppression of caspase-3. C38OX6 (**1**) was generated by the addition of DMP to the broth extracts of actinomycetal strain C38 (Fig. 2A). The preparation scheme of C38OX6 (**1**) is summarized in Figure S1.

Next we attempted to elucidate the structure of C38OX6 (**1**). From HRESI-MS measurements in combination with its ^{1}H and ^{13}C NMR data, the molecular formula of C38OX6 (**1**) was determined to be $C_{27}H_{37}N_3O_2$ (Found: 458.2783 $[M+Na]^+$, Calcd: 458.2783). The molecular formula and ^{1}H and ^{13}C NMR spectra indicated that the structure of C38OX6 (**1**) was quite similar to that of teleocidin B (**2**) (also known as teleocidin B-4 or olivoretin D)[11,12]; therefore, a structural study on C38OX6 (**1**) was performed by comparison with teleocidin B (**2**) (Fig. 2B). The molecular mass of C38OX6 (**1**) (435.60, $C_{27}H_{37}N_3O_2$) was 16 mass units smaller than that of teleocidin B (**2**) (451.64, $C_{28}H_{41}N_3O_2$), corresponding to the loss of CH_4 from teleocidin B (**2**). The UV/vis spectrum of C38OX6 (**1**) (λ_{max}^{MeOH} 232, 283 nm) was almost identical to that of teleocidin B (**2**) (λ_{max}^{MeOH} 231, 286 nm), indicating that they possess the same aglycone (indole).[11] The structure of C38OX6 (**1**) was mainly determined by NMR spectral analyses as follows. The ^{13}C NMR spectrum of C38OX6 (**1**) was quite similar to that of teleocidin B (**2**). Meanwhile, sp^3 methylene (δ 65.0, C-14) and sp^3 methine (δ 56.0, C-9) signals in teleocidin B (**2**) were not observed in C38OX6 (**1**) and a carbonyl carbon (δ 173.6), which does not exist in teleocidin B (**2**), was observed in C38OX6 (**1**). After establishing the direct connectivity between each proton and carbon by the HMQC spectrum, the partial structures in C38OX6 (**1**) were investigated by HMBC experiment. In the HMBC spectrum, ^{1}H–^{13}C long-range couplings from H-8 (δ 3.89 and δ 4.27, isolated methylene) to C-2 (δ 123.9), C-3 (δ 107.1), and C-9 (δ 173.6), and from 10-NH (δ 7.53) to C-8 (δ 38.9) were observed (Fig. 2C). Considering these findings and the molecular formula, the planar structure of C38OX6 (**1**) was determined as shown in Figure 2B. The ^{1}H and ^{13}C NMR spectral data for C38OX6 (**1**) are summarized in Table 1.

The DMP-untreated (control) broth extract of actinomycetal strain C38 contained a significant amount of teleocidin B (**2**), which was decreased in the DMP-treated broth extract (Fig. 2A). This finding raised the possibility that teleocidin B (**2**) was converted into C38OX6 (**1**), at least partly, by the DMP-mediated reaction. To confirm this possibility, purified teleocidin B (**2**) was suspended in CH_2Cl_2 and stirred with DMP in the same manner as the crude broth extract. As a result, C38OX6 (**1**) was detected in this reaction mixture by the LC–PDA–MS system (Fig. S2), indicating that C38OX6 (**1**) was the product generated by DMP-mediated oxidation of C-9 (sp^3 methine) in teleocidin B (**2**) to a carbonyl carbon. C38OX6 (**1**) has three chiral centers (C-12, C-19, and C-22). Since the stereochemistry of teleocidin B (**2**) has already been determined (9*S*, 12*S*, 19*R*, and 22*R*), the stereochemistry of C38OX6 (**1**) was also determined to be [12*S*, 19*R*, and 22*R*] (Fig. 2B).

Teleocidin B (**2**) and its analogs are known to exist mainly in two stable conformers in solution, the *cis* amide in a twist conformation and the *trans* amide in a sofa conformation[13]; however, C38OX6 (**1**) exists in only one conformer in $CHCl_3$ at room temperature. As NOE between H-8 (δ 4.27) and H-12 (δ 4.66) was observed (Fig. 2C), the conformation of C38OX6 (**1**) was determined to be a twist.

2.3. C38OX6 (1) restores XIAP-suppressed enzymatic activity of caspase-3 by inhibition of direct protein–protein interaction

As shown in Figure 3A, C38OX6 (**1**) restored XIAP-suppressed enzymatic activity of caspase-3 at 10 μM without affecting caspase-3 activity in the absence of XIAP. Meanwhile, we could not detect XIAP-inhibitory activity by teleocidin B (**2**), because teleocidin B (**2**) increased caspase-3 activity even in the absence of XIAP (data not shown).

Previous studies showed that XIAP inhibited the enzymatic activities of caspase-3 by direct binding[2]; therefore, we examined whether C38OX6 (**1**) interfered with the binding of XIAP to truncated active caspase-3 using an in vitro GST pull-down assay. Consistent with previous reports, GST-XIAP bound the active form of caspase-3, and this binding was inhibited by C38OX6 (**1**) at over 3 μM (Fig. 3B). This finding suggests that C38OX6 (**1**) interferes with the binding of XIAP to active caspase-3, thereby restoring XIAP-suppressed enzymatic activity of caspase-3. On the other

Table 1
^{13}C and ^{1}H NMR data of C38OX6 (**1**) and teleocidin B (**2**) in $CDCl_3$

Position	C38OX6 (**1**)[a]		Teleocidin B (**2**) (twist conformer)[b]	
	δ_C (ppm)	δ_H (ppm)	δ_C (ppm)	δ_H (ppm)
1		8.83 (1H, br s)		8.67 (1H, br s)
2	123.9	7.01 (1H, d, 1.3)	120.8	6.78 (1H, s)
3	107.1		114.1	
3a	117.3		116.8	
4	145.1		146.0	
5	107.4	6.50 (1H, s)	106.2	6.49 (1H, s)
6	139.7		138.5	
7	119.3		118.0	
7a	138.0		137.8	
8	38.9	3.89 (1H, d, 14.9)	33.7	3.01 (1H, dd, 3.6, 17.2)
		4.27 (1H, d, 14.9)		3.11 (1H, br d, 17.2)
9	173.6		56.0	4.33 (1H, m)
10		7.53 (1H, br s)		7.81 (1H, s)
11	174.5		174.8	
12	73.4	4.66 (1H, d, 10.1)	70.7	4.30 (1H, d, 10.1)
14			65.0	3.56 (1H, m)
				3.72 (1H, m)
15	28.8	2.63 (1H, m)	28.4	2.61 (1H, m)
16	19.9	0.80 (3H, d, 6.6)	19.6	0.68 (3H, d, 6.8)
17	21.8	0.96 (3H, d, 6.2)	21.5	0.91 (1H, d, 6.2)
18	33.0	2.81 (3H, s)	33.0	2.89 (3H, s)
19	40.7		40.0	
20	25.6	1.87*, 1.90* (2H)	24.9	1.4*, 1.9* (2H)
21	35.4	1.87*, 1.90* (2H)	34.8	1.4*, 1.9* (2H)
22	40.3		39.6	
23	29.7	1.31 (3H, s)	29.0	1.34 (3H, s)
24	38.5	2.22 (1H, m)	37.8	2.24 (1H, qq, 6.6, 6.8)
25	17.6	1.00 (3H, d, 6.8)	16.9	1.00 (3H, d, 6.8)
26	18.6	0.53 (3H, d, 6.8)	17.1	0.53 (3H, d, 6.6)
27	22.4	1.50 (3H, s)	21.7	1.50 (3H, s)
28	152.4	6.14 (1H, dd, 10.6, 17.7)	151.8	6.16 (1H, dd, 10.6, 17.6)
29	112.2	5.37 (1H, dd, 1.1, 10.6)	111.3	5.24 (1H, d, 10.6)
		5.43 (1H, dd, 1.1, 17.7)		5.40 (1H, d, 17.6)

Chemical shifts in ppm from TMS as internal standard.
* Obscured by overlapping signals.
[a] Twist (*cis* amide) conformer only (0.04 M, 25 °C).
[b] Twist (*cis* amide) conformer >90% (0.07 M, 24 °C).

hand, teleocidin B (**2**) did not inhibit the binding of GST-XIAP to active caspase-3 (Fig. S3).

2.4. Affinity of C38OX6 (1) for PKC isozymes

It was reported that naturally occurring teleocidin analogs potently bind to and activate protein kinase C (PKC) isozymes, resulting in tumor-promotion.[14,15] Because C38OX6 (**1**) is an analog of teleocidins, we examined whether C38OX6 (**1**) would bind to PKC isozymes. The affinity of C38OX6 (**1**) for each PKC isozyme was evaluated on the basis of inhibition of the specific binding of [^{3}H]phorbol 12,13-dibutyrate (PDBu) to each PKC C1 peptide.[16] As summarized in Table 2, the K_i values of C38OX6 (**1**) for conventional and novel PKC C1 domains were several hundred nanomolars, except that for the PKCδ C1B domain, whose K_i value is 87 nM (Table 2). Meanwhile, teleocidin B (**2**) showed much higher affinity for each PKC isozyme (e.g., K_i value for the PKCα C1A domain was 2.1 nM).

Table 2
K_i values for inhibition of the specific binding of [^{3}H]PDBu by C38OX6 (**1**)

PKC C1 peptides[a]	K_i (nM) C38OX6 (**1**)	K_d (nM) [^{3}H]PDBu[b]
α-C1A	600 (40)[c]	1.1
β-C1A	730 (50)	1.3
γ-C1A	660 (40)	1.5
δ-C1B	87 (5)	0.53
ε-C1B	480 (60)	0.81
η-C1B	360 (40)	0.45

[a] The C1A domains of conventional PKCs (α, β, and γ) are mainly involved in phorbol ester binding and translocation from the cytosol to plasma membrane (Refs. 27,28), whereas the C1B domains of novel PKCs (δ, ε, and η) play a critical role in translocation in response to the phorbor ester TPA (Ref. 29). Our binding data using PKC C1 peptides supports these data; the major binding sites of indolactam-V, the core structure of teleocidins, are the C1A domains of conventional PKCs and the C1B domains of novel PKCs (Ref. 30). Therefore, we used the C1A peptides of conventional PKCs and the C1B peptides of novel PKCs to evaluate the binding affinity for PKC isozymes of our compounds.
[b] Ref. 25.
[c] Standard deviation from triplicate experiments.

2.5. C38OX6 (1) sensitizes cancer cells to anticancer drugs

Previous studies showed that knockdown of XIAP using antisense oligonucleotides sensitized cancer cells to conventional anticancer drugs.[17] We also performed RNAi experiments to investigate whether the loss of XIAP could sensitize human cervical carcinoma HeLa cells to anticancer drugs. The successful knockdown of XIAP by siRNA was confirmed by immunoblotting (Fig. 4A). We confirmed that specific siRNA for XIAP sensitized HeLa cells to camptothecin or staurosporine (Fig. 4A). We therefore examined whether our XIAP inhibitor could also sensitize HeLa cells to camptothecin or staurosporine. As shown in Figure 4B, apoptosis induced by camptothecin or staurosporine was significantly promoted by co-treatment with C38OX6 (**1**) in HeLa cells. These results were further

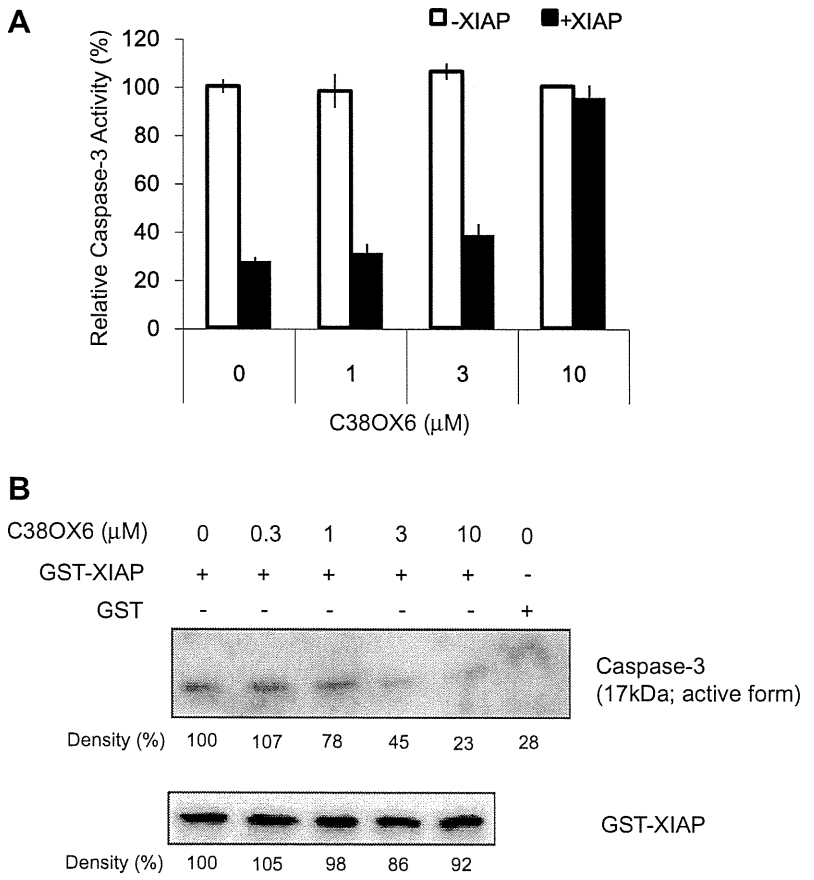

Figure 3. C38OX6 (**1**) interfered with the interaction between XIAP and caspase-3. (A) Effects of C38OX6 (**1**) on XIAP-suppressed caspase-3 activity. Recombinant active caspase-3 and C38OX6 (**1**) were mixed and incubated for 1 h at 37 °C in the presence or absence of GST-XIAP. Activity of caspase-3 was measured by the fluorogenic substrate Ac-DEVD-AFC. Values are the means of three independent determinations. Bars, SD. (B) Effects of C38OX6 (**1**) on the binding of XIAP to active caspase-3. Glutathione-Sepharose 4B beads, GST-XIAP (or GST), and active caspase-3 were incubated with C38OX6 (**1**) at 4 °C for 1 h. After washing, bound proteins were separated by SDS–PAGE followed by immunoblotting with anti-caspase-3 and anti-GST antibodies.

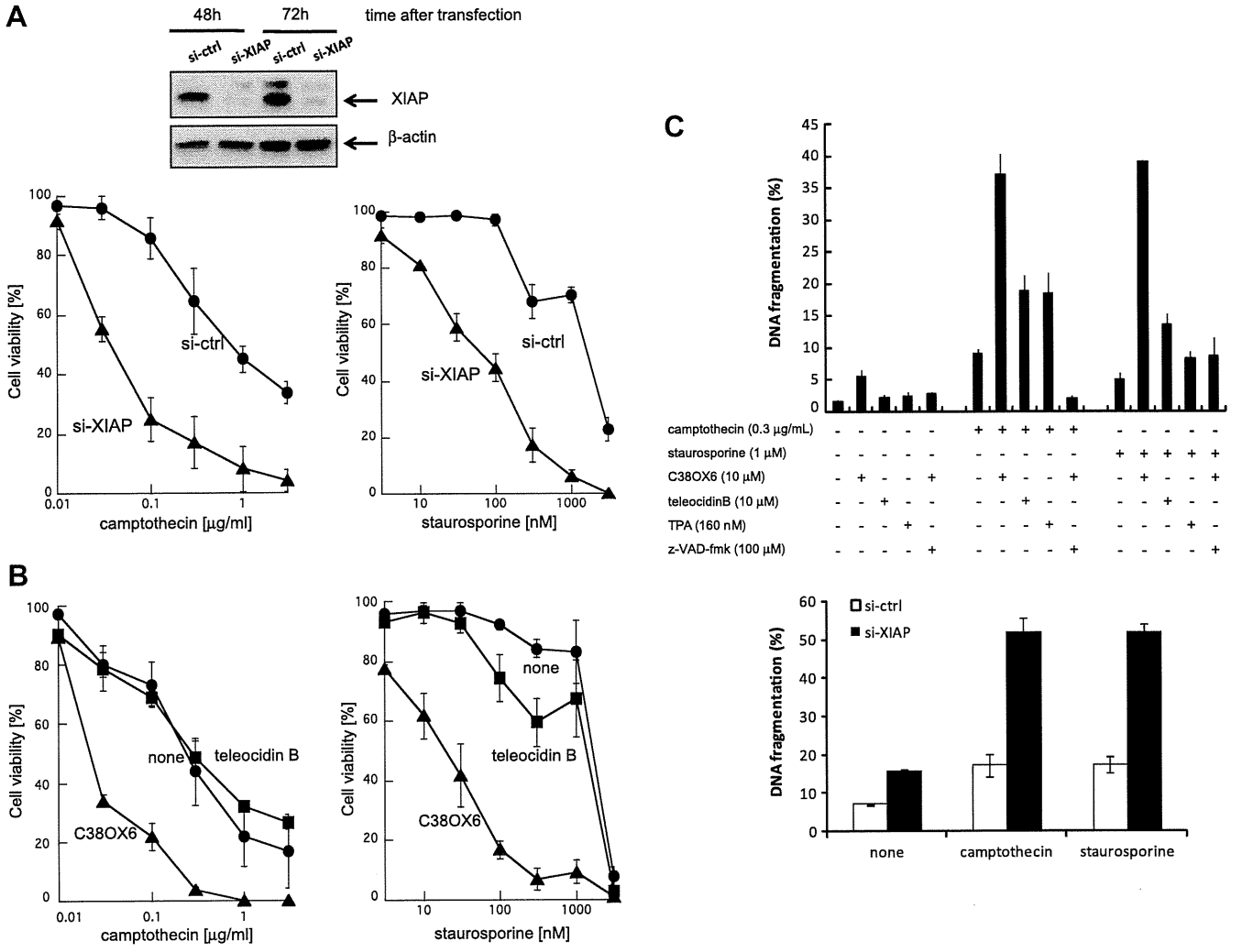

Figure 4. Effects of C38OX6 (**1**) on the sensitivity of cancer cells to anticancer drugs. (A) HeLa cells were transfected with XIAP or control siRNA 48 h before treatment of camptothecin. After 48 h of chemical treatment, cell viability was determined by trypan blue dye exclusion assay (bottom). Expression levels of XIAP and β-actin were examined by SDS–PAGE and immunoblotting (top). (B) HeLa cells were treated for 48 h with indicated concentrations of camptothecin or staurosporine in the presence or absence of test compounds (10 μM). Cell viability was determined by trypan blue dye exclusion assay. (C) HeLa cells were treated for 24 h with camptothecin (0.3 μg/mL) or staurosporine (1 μM) in the presence or absence of test compounds (top). HeLa cells were transfected with XIAP or control siRNA 48 h, followed by chemical treatment (bottom). Cell viability was determined by FACS analysis of DNA fragmentation of propidium iodide-stained nuclei (sub-G1 population was measured). Values are the means of three independent determinations. Bars, SD.

confirmed by propidium iodide-staining assay. As shown in Figure 4C, treatment of HeLa cells with C38OX6 (**1**) in the presence of camptothecin or staurosporine induced DNA fragmentation. This DNA fragmentation was suppressed by z-VAD-fmk, a pan-caspase inhibitor (Fig. 4C), indicating that C38OX6 (**1**) and the anticancer drug synergistically induced caspase-dependent apoptosis. To exclude the possibility that this apoptosis-enhancing effect of C38OX6 (**1**) is due to its weak but still retained PKC-binding ability, teleocidin B was examined for its ability to enhance anticancer drug-induced apoptosis. As shown in Fig. 4B and C, significant synergistic effects of teleocidin B with camptothecin or staurosporine were not observed in HeLa cells. In addition, 12-*O*-tetradecanoylphorbol-13-acetate (TPA), a phorbol ester-type tumor promoter that is known to activate PKC isozymes, did not sensitize HeLa cells to camptothecin and staurosporine at the effective dose range for PKC activation (Fig. 4C). These results suggest that C38OX6 (**1**) sensitized HeLa cells to anticancer drug-induced apoptosis, possibly due to its inhibitory effect on the anti-apoptotic function of XIAP, but not due to the activation of PKC.

3. Discussion

Historically, a number of bioactive natural products, such as antibiotics, antimalarials, immunosuppressants, and anticancer drugs, have revolutionized medicine. Indeed, among all available anticancer drugs from around the 1940s to 2006, 14% were natural products and 28% were natural product derivatives,[18] indicating that natural products and their derivatives are still high-quality sources for drug-lead discovery. Therefore, in the present study, we focused on the generation and use of a new chemical library consisting of chemically modified microbial metabolites which are referred to as 'Unnatural Natural Products (UNPs)'.

To generate the UNP library, we devised and developed a series of unique procedures via the addition of chemical reagents to crude microbial broth extracts combined with the detection and purification of reaction products (UNPs) by the LC–PDA–MS system. In these procedures, the reaction conditions of chemical conversion were quite important factors because each actinomycetal strain produces different secondary metabolites and some metabolites

are unstable at extreme temperature and pH. However, we established the broadly applicable reaction conditions after several examinations and, using our established method, generated an UNP library consisting of various types of compounds, such as trieneansamycin compounds, polyene-macrolide compounds, anthraquinone compounds and so on.

For the construction of chemical libraries consisting of natural product analogs, several approaches have been reported. One of the most intensively researched approaches is combinatorial biosynthesis, especially using modular polyketide synthases (PKSs) and non-ribosomal peptide synthetases (NRPSs), which are large multidomain enzymes sequentially condensing short fatty acids and α-amino acids, respectively.[19] For example, the 'Unnatural Natural Product library' consisting of polyketides was constructed by multiple genetic modifications of 6-deoxyerythronolide B synthase, the PKS, which produces the macrolide ring of erythromycin.[20] As another unique approach, genetic code reprogramming by a ribozyme-based de novo tRNA acylation system combined with a cell-free translation system enabled the generation of natural product-like non-standard peptides.[21] Compared with the above approaches, chemical conversion is a simple and somewhat classical approach for generating natural product analogs, and is applicable to various types of compounds. In addition, the combination of chemical conversion of microbial metabolites in crude broth extracts and purification by the LC–PDA–MS system enabled us to effectively generate the UNP library.

In addition to developing the UNP library, we also aimed to utilize it. In the course of screening for unique bioactive compounds by several in-house assay systems, C38OX6 (**1**) was identified as a new inhibitor of XIAP. C38OX6 (**1**) abrogated the interaction between XIAP and active caspase-3, thereby restoring XIAP-suppressed enzymatic activity of caspase-3 (Fig. 3A and B). Similarly, two types of compounds, aryl sulfonamide compounds and polyphenylurea compounds, were previously reported as XIAP inhibitors which interfered with the binding of XIAP to caspase-3.[10,22] In the same manner as treatment of polyphenylurea compounds, C38OX6 (**1**) sensitized cancer cells to anticancer drugs (Fig. 4B and C), and the effective concentration of C38OX6 (**1**) in cells was approximately the same degrees as in aryl sulfonamide compounds and polyphenylurea compounds.

We confirmed that C38OX6 (**1**) was a reaction product generated by DMP-mediated conversion of teleocidin B (**2**). As teleocidin B (**2**) is known to exhibit tumor-promoting activity by potent binding to and activation of several PKC isozymes,[15] it is noteworthy that the affinity of C38OX6 (**1**) for each PKC isozyme was significantly decreased as compared to that of telocidin B (K_i value for the PKCα C1A domain was 2.1 nM; Table 2). A methine carbon (C-9) linked to a hydroxymethyl group in teleocidin B (**2**) was changed into a carbonyl carbon in C38OX6 (**1**). These findings are consistent with a previous report that a free hydroxyl group at C-14 was important for the tumor-promoting activity of teleocidin B (**2**).[23] Although the affinity of C38OX6 (**1**) for conventional and novel PKC isozymes was much lower than that of teleocidin B (**2**), we could not completely reject the involvement of some PKC isozymes in sensitization to anticancer drugs by C38OX6 (**1**). However, potent PKC activators, teleocidin B (**2**) and TPA, failed to sensitize HeLa cells to anticancer drugs at effective concentrations for PKC activation (Fig. 4B and C). These results strongly suggest that C38OX6 (**1**) sensitizes cancer cells to anticancer drugs by its XIAP-inhibitory activity, but not in a PKC-dependent manner. After structure–activity relationship study of C38OX6 (**1**) for complete removal of PKC activation and increased XIAP inhibition, a new class of anticancer drugs that inhibit XIAP will be developed.

In the DMP-treated broth extract of actinomycetal strain C38, several teleocidin-like UNPs judged from their physico-chemical properties were detected. However, all tested teleocidin-like UNPs other than C38OX6 (**1**) did not inhibit the anti-apoptotic function of XIAP like teleocidin B (**2**) (data not shown).

This study suggests that UNPs are superior to their original natural products in cases such as C38OX6 (**1**), and generation of the UNP library is a promising approach to increase the diversity of sources and obtain unique bioactive compounds for drug development.

4. Conclusion

In the present study, we generated a new chemical library consisting of chemically modified microbial metabolites which are referred to as 'Unnatural Natural Products (UNPs)' through a series of procedures via chemical conversion of microbial metabolites in crude broth extracts followed by purification of reaction products with the LC–PDA–MS system. Using our UNP library, we discovered an XIAP inhibitor, C38OX6 (**1**), which interfered with the binding of XIAP to caspase-3, thereby restoring XIAP-suppressed enzymatic activity of caspase-3 in vitro. Furthermore, C38OX6 (**1**) was found to sensitize cancer cells to anticancer drugs.

5. Material and methods

5.1. General experimental procedure. Fermentation of actinomycetes and preparation of broth extracts, preparation of C38OX6 (1) and teleocidin B (2)

See 'Supplementary data' section.

5.2. Cell culture

Human cervical carcinoma HeLa cell line was cultured in DMEM containing 8% fetal bovine serum, 2.5 g/L sodium bicarbonate, penicillin G (100 units/mL), and kanamycin (0.1 g/L).

5.3. Caspase de-repression assay

The caspase de-repression assay was performed as described previously with several modifications.[10] Briefly, cDNA of full-length human XIAP was cloned from HeLa cells and inserted as an EcoRI fragment into the pGEX-2T vector (GE Healthcare, NJ), and recombinant GST-XIAP was produced in *Escherichia coli* and purified. Recombinant human active caspase-3 (0.01 unit; Enzo Life Sciences, NY), recombinant GST-XIAP (100 ng), a test compound, and the fluorogenic tetrapeptide substrate acetyl-Asp-Glu-Val-Asp-[7-amino-4-trifluoromethylcoumarin](Ac-DEVD-AFC, 10 μM; Enzo Life Sciences) were mixed and incubated in caspase assay buffer (20 mM Tris, 100 mM NaCl, 10 mM DTT, and 3% glycerol, pH 7.5) for 1 h at 37 °C after preincubation for 30 min at 30 °C without the fluorogenic substrate. The activity of caspase-3 was measured by monitoring the cleavage of Ac-DEVD-AFC using a spectrofluorometric plate reader at excitation and emission wavelengths of 405 and 510 nm, respectively.

5.4. GST pull-down assay

Recombinant GST-XIAP (or GST) (1 μg), recombinant human active caspase-3, and 10 μL Glutathione-Sepharose 4B beads (GE Healthcare) were incubated at 4 °C for 1 h in 1 mL of caspase assay buffer in the presence or absence of a test compound. After three washes, the bound proteins were separated by SDS–PAGE, followed by immunoblotting with the primary antibodies against caspase-3 (sc-7148; Santa Cruz, CA) or GST (sc-138; Santa Cruz).

5.5. [^{3}H]PDBu-binding assay

The binding of [^{3}H]PDBu to PKC C1 peptides was evaluated using the procedure of Sharkey and Blumberg[24] with modifications

as reported previously[25] with 50 mM Tris-maleate buffer (pH 7.4 at 4 °C), 10–40 nM PKC C1 peptide, 20 nM [^{3}H]PDBu (16.3 Ci/mmol), 50 μg/mL 1,2-dioleoyl-*sn*-glycero-3-phospho-L-serine, 3 mg/mL bovine γ-globulin, and various concentrations of inhibitor. Binding affinity was evaluated on the basis of the concentration required to cause 50% inhibition of the specific binding of [^{3}H]PDBu, IC_{50}, which was calculated with PriProbit 1.63 software.[26] The inhibition constant K_i was calculated using the method of Sharkey and Blumberg.[24] Although we used each PKC C1 peptide in the range 10–40 nM, the concentration of the properly folded peptide was estimated to be about 3 nM based on the B_{max} values of the Scatchard analyses reported previously[25]; therefore, the concentration of free PDBu will not markedly vary over the dose–response curve.

5.6. Knockdown of XIAP using siRNA

siRNA for XIAP (HSS100565) and the control (12935-112) were purchased from Invitrogen (CA), and were transfected into cells using Lipofectamine RNAi MAX (13778150, Invitrogen). After 48 h of transfection of each siRNA, test compounds were treated, followed by cell death assay. Expression levels of XIAP and β-actin (loading control) were examined by SDS–PAGE and immunoblotting with the primary antibodies against XIAP (610762; BD Biosciences Pharmingen, CA) and β-actin (A5316; Sigma–Aldrich, MO).

5.7. Cell death assay

HeLa cells were seeded at 2×10^4 cells/well in 48-well plates and cultured overnight. The cells were treated with various concentrations of test compounds for 48 h. Cell viability was counted by trypan blue dye exclusion assay (Fig. 4A and B). HeLa cells were seeded at 1×10^5 cells/well in 12-well plates and cultured overnight. The cells were treated with various concentrations of test compounds for 24 h. Subsequently, cells were stained with propidium iodide, followed by determination of cell death by fluorescence-activated cell sorting (FACS) analysis (Epics Altra; Beckman Coulter, CA) of DNA fragmentation of propidium iodide-stained nuclei (sub-G1 population was measured) (Fig. 4C). z-VAD-fmk was purchased from Sigma–Aldrich (MO).

Acknowledgments

We are grateful to T. Watabe, Y. Fujimoto, and Y. Matsui (Keio University) for help with construction of the UNP library. This study was supported in part by a 2009 Innovative Research Program Award from the Japanese Society of Bioscience, Biotechnology, and Agrochemistry (JSBBA). T.K. was a research assistant for the Global COE Program for Human Metabolomic Systems Biology.

Supplementary data

Supplementary data associated with this article can be found, in the online version, at doi:10.1016/j.bmc.2011.05.009. These data include MOL files and InChiKeys of the most important compounds described in this article.

References and notes

1. LaCasse, E. C.; Mahoney, D. J.; Cheung, H. H.; Plenchette, S.; Baird, S.; Korneluk, R. G. *Oncogene* **2008**, *27*, 6252.
2. Deveraux, Q. L.; Takahashi, R.; Salvesen, G. S.; Reed, J. C. *Nature* **1997**, *388*, 300.
3. Deveraux, Q. L.; Roy, N.; Stennicke, H. R.; Van Arsdale, T.; Zhou, Q.; Srinivasula, S. M.; Alnemri, E. S.; Salvesen, G. S.; Reed, J. C. *EMBO J.* **1998**, *17*, 2215.
4. Deveraux, Q. L.; Leo, E.; Stennicke, H. R.; Welsh, K.; Salvesen, G. S.; Reed, J. C. *EMBO J.* **1999**, *18*, 5242.
5. Harlin, H.; Reffey, S. B.; Duckett, C. S.; Lindsten, T.; Thompson, C. B. *Mol. Cell. Biol.* **2001**, *21*, 3604.
6. Li, J. W.; Vederas, J. C. *Science* **2009**, *325*, 161.
7. Feher, M.; Schmidt, J. M. *J. Chem. Inf. Comput. Sci.* **2003**, *43*, 218.
8. Abel, U.; Koch, C.; Speitling, M.; Hansske, F. G. *Curr. Opin. Chem. Biol.* **2002**, *6*, 453.
9. Liu, X.; Ashforth, E.; Ren, B.; Song, F.; Dai, H.; Liu, M.; Wang, J.; Xie, Q.; Zhang, L. *J. Antibiot.* **2010**, *63*, 415.
10. Schimmer, A. D.; Welsh, K.; Pinilla, C.; Wang, Z.; Krajewska, M.; Bonneau, M. J.; Pedersen, I. M.; Kitada, S.; Scott, F. L.; Bailly-Maitre, B., et al *Cancer Cell* **2004**, *5*, 25.
11. Sakai, S.; Aimi, N.; Yamaguchi, K.; Hitotsuyanagi, Y.; Watanabe, C.; Yokose, K.; Koyama, Y.; Shudo, K.; Itai, A. *Chem. Pharm. Bull.* **1984**, *32*, 354.
12. Hitotsuyanagi, Y.; Fujiki, H.; Suganuma, M.; Aimi, N.; Sakai, S.; Endo, Y.; Shudo, K.; Sugimura, T. *Chem. Pharm. Bull.* **1984**, *32*, 4233.
13. Irie, K.; Isaka, T.; Iwata, Y.; Yanai, Y.; Nakamura, Y.; Koizumi, F.; Ohigashi, H.; Wender, P. A.; Satomi, Y.; Nishino, H. *J. Am. Chem. Soc.* **1996**, *118*, 10733.
14. Fujiki, H.; Suganuma, M.; Matsukura, N.; Sugimura, T.; Takayama, S. *Carcinogenesis* **1982**, *3*, 895.
15. Fujiki, H.; Sugimura, T. *Adv. Cancer Res.* **1987**, *49*, 223.
16. Irie, K.; Oie, K.; Nakahara, A.; Yanai, Y.; Ohigashi, H.; Wender, P. A.; Fukuda, H.; Konishi, H.; Kikkawa, U. *J. Am. Chem. Soc.* **1998**, *120*, 9159.
17. Hu, Y.; Cherton-Horvat, G.; Dragowska, V.; Baird, S.; Korneluk, R. G.; Durkin, J. P.; Mayer, L. D.; LaCasse, E. C. *Clin. Cancer Res.* **2003**, *9*, 2826.
18. Newman, D. J.; Cragg, G. M. *J. Nat. Prod.* **2007**, *70*, 461.
19. Weissman, K. J.; Müller, R. *Chembiochem* **2008**, *9*, 826.
20. McDaniel, R.; Thamchaipenet, A.; Gustafsson, C.; Fu, H.; Betlach, M.; Ashley, G. *Proc. Natl. Acad. Sci. U.S.A.* **1999**, *96*, 1846.
21. Murakami, H.; Ohta, A.; Ashigai, H.; Suga, H. *Nat. Methods* **2006**, *3*, 357.
22. Wu, T. Y.; Wagner, K. W.; Bursulaya, B.; Schultz, P. G.; Deveraux, Q. L. *Chem. Biol.* **2003**, *10*, 759.
23. Horiuchi, T.; Fujiki, H.; Suganuma, M.; Hakii, H.; Nakayasu, M.; Hitotsuyanagi, Y.; Aimi, N.; Sakai, S.; Endo, Y.; Shudo, K., et al *Gann* **1984**, *75*, 837.
24. Sharkey, N. A.; Blumberg, P. M. *Cancer Res.* **1985**, *45*, 19.
25. Shindo, M.; Irie, K.; Nakahara, A.; Ohigashi, H.; Konishi, H.; Kikkawa, U.; Fukuda, H.; Wender, P. A. *Bioorg. Med. Chem.* **2001**, *9*, 2073.
26. Sakuma, M. *Appl. Entomol. Zool.* **1998**, *33*, 339.
27. Raghunath, A.; Ling, M.; Larsson, C. *Biochem. J.* **2003**, *370*, 901.
28. Quest, A. F. G.; Bell, R. M. *J. Biol. Chem.* **1994**, *269*, 20000.
29. Szallasi, Z.; Bogi, K.; Gohari, S.; Biro, T.; Acs, P.; Blumberg, P. M. *J. Biol. Chem.* **1996**, *271*, 18299.
30. Masuda, A.; Irie, K.; Nakagawa, Y.; Ohigashi, H. *Biosci., Biotechnol., Biochem.* **2002**, *66*, 1615.